Journal of Experimental Psychology: General

Extending Continuous Flow Models of Immediate Decision Reports to Delayed Decision Reports

Johan A. Achard, Thibault Gajdos Preuss, and Mathieu Servant

Online First Publication, April 10, 2025. https://dx.doi.org/10.1037/xge0001748

AMERICAN PSYCHOLOGICAL ASSOCIATION

Journal of Experimental Psychology: General

ISSN: 0096-3445

https://doi.org/10.1037/xge0001748

Extending Continuous Flow Models of Immediate Decision Reports to Delayed Decision Reports

Johan A. Achard[1, 2], Thibault Gajdos Preuss[3], and Mathieu Servant[1, 2]

[1] Laboratoire de Recherches Intégratives en Neurosciences et Psychologie Cognitive, Institut National de la Santé et de la Recherche Médicale, Université Marie et Louis Pasteur

[2] Maison des Sciences de l'Homme et de l'Environnement, Centre National de la Recherche Scientifique, Université Marie et Louis Pasteur

[3] Centre de Recherche en Psychologie et Neuroscience, Centre National de la Recherche Scientifique, Aix-Marseille Université

Continuous flow and evidence accumulation models have recently been combined to provide an integrated account of decision and motor mechanisms engaged in choice reaction time tasks. According to this account, muscle activation is essentially determined by the evidence accumulation decision variable through a continuous decision-to-motor transmission of information. However, it remains unclear whether and how this framework can be extended to situations that impose a time lag between the commitment to a choice and the expression of that choice through actions. Such situations have been studied using response signal (RS) decision tasks featuring a short delay between the offset of the stimulus and a signal to respond. The present work integrates recent developments in decision-making, working memory, and motor control research to extend models of immediate decision reports to delayed decision reports. We assumed that the evidence accumulation decision variable transitions to sustained activity after hitting a threshold to achieve the short-term maintenance of the selected choice. The level of sustained activity then constitutes the starting point for a second phase of accumulation, in which subjects sample evidence from the RS to activate the muscles. We tested predictions from the theory at the behavioral and muscle activation levels in three RS decision tasks featuring manipulations of stimulus duration, delay duration, and foreknowledge of the stimulus–response mapping. Muscle activation was measured using electromyography. The theory provided a unified account of empirical effects.

Public Significance Statement

Goal-directed behavior requires a translation of decisions into actions, and psychological research has offered sophisticated models of this process. However, their scope is limited to decisions that are immediately followed by actions, while many real-life situations require a short delay between them. For example, imagine a child raising one's hand while waiting for the teacher's signal to respond, or a basketball player preparing to shoot a 3-point goal and waiting to receive the ball. The present work builds on recent neuroscience findings suggesting common mechanisms for the decision process and the short-term maintenance of the choice to propose a novel theoretical account of delayed decision reports.

Keywords: decision-making, evidence accumulation, working memory, motor control, electromyography

Jared Medina served as action editor.

Mathieu Servant https://orcid.org/0000-0002-1864-5881

Thibault Gajdos Preuss and Mathieu Servant share the senior authorship. The empirical data and python codes to run the experiments and process the data are available on the Open Science Framework at https://osf.io/vf95p/. Views and opinions expressed are those of the authors only and do not necessarily reflect those of the European Union or the European Research Council. Neither the European Union nor the granting authority can be held responsible for them. Some of the data and ideas appearing in this article have been presented at the 2023 Annual Meeting of the Psychonomic Society.

The authors declare no conflicts of interest. This research was funded in whole, or in part, by the European Commission (Grant 101039226). For the purpose of open access, the author has applied a CC BY public copyright license to any Author Accepted Manuscript version arising from this submission.

Johan A. Achard played a lead role in investigation and visualization and an equal role in conceptualization, data curation, formal analysis, methodology, software, writing–original draft, and writing–review and editing. Thibault Gajdos Preuss played a supporting role in supervision and an equal role in conceptualization, formal analysis, methodology, writing–original draft, and writing–review and editing. Mathieu Servant played a lead role in funding acquisition, project administration, resources, and supervision, a supporting role in investigation and visualization, and an equal role in conceptualization, data curation, formal analysis, methodology, software, writing–original draft, and writing–review and editing.

Correspondence concerning this article should be addressed to Mathieu Servant, Laboratoire de Recherches Intégratives en Neurosciences et Psychologie Cognitive, Institut National de la Santé et de la Recherche Médicale, Université Marie et Louis Pasteur, Unité de Formation et de Recherche Santé, bâtiment Rabelais, 19 rue Ambroise Paré, 25030 Besançon Cedex, France. Email: mathieu.servant@univ-fcomte.fr

A growing body of experimental and theoretical work suggests that decisions and actions can be closely intertwined. In particular, in situations where decisions lead to immediate actions, behavioral studies and electrophysiological investigations of the motor system have revealed a continuous transmission of the evolving decision variable to the motor structures that prepare and execute the response (Buc Calderon et al., 2015; Chapman et al., 2010; Coles, 1989; Eriksen et al., 1985; Gold & Shadlen, 2000, 2007; Hanes & Schall, 1996; Heitz & Schall, 2012; Kinder et al., 2022; Nakayama et al., 2023; O'Connell & Kelly, 2021; Reppert et al., 2018; Schall, 2019; Servant et al., 2015, 2021; Song & Nakayama, 2009; Thura, 2020; Thura & Cisek, 2014, 2016). These results have provided the foundation for theoretical models in which decisions and actions are driven by common mechanisms, through a continuous flow of information (Calderon et al., 2018; Eriksen & Eriksen, 1979; McClelland, 1979). Formal characterizations of these mechanisms have been proposed (Balsdon et al., 2023; Cisek et al., 2009; Dendauw et al., 2024; Friedman et al., 2013; Lepora & Pezzulo, 2015; Purcell et al., 2010, 2012; Servant et al., 2015, 2019, 2021; Thura et al., 2012; Verdonck et al., 2021), but extending the models to situations where decisions are not immediately followed by actions is not straightforward. Progressing on this issue is important, because the decoupling of decision and action is a common occurrence in real life, and greatly contributes to the flexibility of human behavior. Such decoupling can operate on short (e.g., a child in class who raises one's hand while waiting for the teacher's signal to respond) or long (e.g., deciding to quit a job, deciding to vote for a candidate in a presidential election) timescales.

The present work draws upon current scientific knowledge on the relationship between decision-making, memory, and motor systems to extend continuous flow models of immediate decision reports to delayed decision reports. Due to the constraints of experimental methods and the use of electrophysiology, we limit our investigations to delays that operate on relatively short timescales. The remainder of the introduction is structured as follows. We first introduce current continuous flow models of immediate decision reports. We then review empirical work on delayed decision reports, and discuss how continuous flow models could be extended to these situations, given our current state of knowledge. We finally derive general predictions from this extended framework, which will be tested in three experiments.

Continuous Flow Models of Immediate Decision Reports

In experimental psychology, immediate decision reports have traditionally been studied using tasks in which participants are instructed to choose between two or more responses based on a stimulus attribute. We refer to these tasks as free response (FR) tasks, because the response time (RT) is controlled by the subject, and is defined as the latency between the onset of the stimulus and the response. Sequential sampling decision models have been developed since the 1960s to explain RT distributions and choice probabilities observed in FR tasks (e.g., LaBerge, 1962; Laming, 1968; Stone, 1960). According to these models, decision-making builds upon an accumulation of noisy samples of evidence until a threshold is reached (one threshold for each response; for reviews, see Forstmann et al., 2016; Ratcliff & Smith, 2004; Ratcliff, Smith, et al., 2016). The evidence may come from various sources, such as sensory inputs and memory stores. The average quality of evidence determines the accumulation rate, with lower rates producing slower and more error-prone decisions.

More recently, sequential sampling models have received empirical support from single-unit recordings in behaving monkeys (for reviews, see Gold & Shadlen, 2007; Hanks & Summerfield, 2017; Schall, 2019). In humans, electroencephalographic (EEG) and magnetoencephalographic studies have identified two classes of signals with the same properties as the theoretical accumulation-to-threshold decision variable (for reviews, see Kelly & O'Connell, 2015; O'Connell & Kelly, 2021). The first class of signals corresponds to the centroparietal positivity and reflects stimulus categorization. It is fully independent from the motor requirements of the task and appears even when subjects are instructed to make the decision mentally (e.g., O'Connell et al., 2012; Twomey et al., 2015). The second class of signals, maximal over motor areas, corresponds to classic effector-selective motor preparation activities such as the lateralized readiness potential (e.g., Gluth et al., 2013; Kelly & O'Connell, 2013; Lui et al., 2021; Servant et al., 2016) and the decrease in spectral activity in the μ/β band (e.g., de Lange et al., 2013; Donner et al., 2009; Kelly et al., 2021; O'Connell et al., 2012; Rogge et al., 2022; Steinemann et al., 2018; Twomey et al., 2016). Both signals exhibit a rise-to-threshold morphology, with a rising slope modulated by the quality of evidence, and a peak amplitude around the time of the response. Importantly, the two signals largely evolve in parallel, with the onset of the motor preparation signal slightly lagging the onset of the stimulus categorization signal (Kelly & O'Connell, 2013).

To account for these findings, recent extensions of sequential sampling models distinguish two evidence accumulation processes (Dendauw et al., 2024; Verdonck et al., 2021). In order to make the present article as simple and accessible as possible, we will focus on general conceptual aspects of the models,[1] and FR tasks that require a choice between two manual responses (left and right). The first evidence accumulation process $x(t)$ is assumed to perform a decision about the category of the stimulus. It is modeled as a one-dimensional diffusion process, according to which evidence for one-stimulus category constitutes evidence against the other category. If there is no bias toward a specific category, $x(t)$ starts at 0. Positive evidence favors stimulus category A, while negative evidence favors stimulus category B. Variable $x(t)$ is continuously transmitted to motor preparation brain areas, but can be corrupted by noise in neural networks during the transmission process. The motor preparation process $y(t)$ approximates a particular type of filter, known as the Kalman-Bucy filter, to optimally recover $x(t)$ from noise. Variable $y(t)$ thus corresponds to a smoothed and lagged version of $x(t)$, with the lag arising from the filter.[2] The filter also introduces a slight nonlinearity in the accumulation rate, but these properties will not be considered further in the context of the present work, given that they will not have any meaningful impact on predictions. However, it is important to recognize that a decrease in the quality of evidence will produce a reduction in the accumulation rate of both $x(t)$ and $y(t)$. If there is no bias toward a particular response category, $y(t)$ starts

[1] A full mathematical specification of the models is available in Verdonck et al. (2021) and Dendauw et al. (2024).

[2] Evidence for a filtering mechanism at the motor preparation level comes from model fits to behavioral and electrophysiological data in FR tasks (Balsdon et al., 2023; Dendauw et al., 2024; Verdonck et al., 2021).

at 0, with positive evidence favoring the right-hand response, and negative evidence favoring the left-hand response.

This extended sequential sampling model framework has been further refined to account for motor phenomena occurring at the muscular level, as revealed by surface EMG recordings. Because EMG is relatively uncommon in experimental psychology compared to EEG and magnetoencephalographic techniques, and considering our utilization of EMG in the present work, it is important to provide a comprehensive overview of its principles. EMG measures myoelectric activity produced by muscles in response to neural excitation, using two or more electrodes placed on the skin surface, above the targeted muscle(s). When the EMG baseline is zero, which is typically achieved by applying a high-pass filter to the signal (to remove slow drifts unrelated to muscular activity), muscle activation is reflected by a burst of positive and negative voltage deflections, operating on a shorter timescale than RT. To ensure that the EMG signal does not average to zero, researchers typically consider the (full-wave) rectified EMG signal, obtained by taking the absolute value of voltages across time points. The amplitude of a rectified EMG burst reflects global muscle activation and is highly correlated to force production (for a review, see Vigotsky et al., 2018).[3] On average, it takes the form of a ramping activity that peaks around the time of the response. When the quality of evidence decreases, the slope of this ramping activity also decreases on average, producing a slower mean motor time (defined as the mean latency between the onset of muscle activation and the response; Dendauw et al., 2024; Servant et al., 2021). These properties are reminiscent of the theoretical evidence accumulation variable.

To account for these findings, Dendauw et al. (2024) hypothesized that the motor preparation variable $y(t)$ is gated prior to activating muscle fibers. The gate, presumably mediated by the basal ganglia system and spinal circuits, is modeled as a constant inhibition applied to $y(t)$. Formally, inputs to left and right muscle fibers, variables $z_L(t)$ and $z_R(t)$ respectively, are defined as follows:

$$\begin{cases} Z_L(t) = \max(-y(t) - g, 0) \\ Z_R(t) = \max(y(t) - g, 0) \end{cases}, \quad (1)$$

where parameter g corresponds to gating inhibition. Thus, the motor preparation variable $y(t)$ is transmitted to muscle fibers if and only if it exceeds a particular level of activation, determined by parameter g. This gating mechanism saves muscular effort by preventing low levels of motor preparation from activating muscle fibers and protects the system against unwanted motor impulses.

The electrical activation of muscle fibers, measured by EMG, starts when $z_L(t)$ or $z_R(t) > 0$. A response (button press) is produced when muscle activation reaches a threshold level (parameter θ_{resp}, referred to as response threshold), primarily determined by the force required to respond and muscle properties. A left response is produced if $z_L(t)$ first reaches the response threshold, while a right response is produced if $z_R(t)$ first reaches the response threshold. Because the rectified EMG signal covaries with $z_L(t)$ and $z_R(t)$, the model provides a straightforward explanation of empirical EMG findings. When the quality of evidence decreases, the accumulation rate of the motor preparation variable decreases, which produces a decrease in the muscle activation slope on average. This architecture has been termed *gated cascade diffusion model* (GCD) to emphasize the main processing components (diffusion decision variable, continuous flow, and gate). A simplified schematic of the model is provided in Figure 1A. The schematic illustrates the expected mean of motor preparation and muscle activation trajectories for two conditions, involving high and low quality of evidence, respectively.

Besides mean activation dynamics, GCD predicts a particular muscle phenomenon at the single-trial level. Noisy fluctuations of the motor preparation variable $y(t)$ can sometimes produce *partial* muscle activations that do not lead to a response. This phenomenon occurs when $z_L(t)$ or $z_R(t) > 0$ for a short period without reaching the response threshold θ_{resp} (Figure 1B). The predicted rate of partial muscle activation in the EMG channel associated with the response increases as the quality of evidence decreases, due to the underlying decrease in the signal-to-noise ratio of the motor preparation variable $y(t)$. This prediction has been validated (Dendauw et al., 2024; Servant et al., 2021). Empirical illustrations of partial muscle activations are provided in Appendix A.

Delayed Decision Reports

Delayed decision reports have been studied in both monkeys and humans using response signal (RS) decision tasks. RS tasks are similar to FR tasks, except that subjects are instructed to respond when a RS, controlled by the experimenter, appears on the screen. Consequently, the RT is defined as the latency between RS onset and the response. The main parameters of RS tasks are (a) stimulus presentation duration, (b) RS latency relative to stimulus onset, (c) presence of a delay between stimulus offset and RS onset, and (d) knowledge of the stimulus–response mapping during stimulus presentation. Because our interest is in delayed decision reports, we shall focus on studies that used a relatively long RS latency relative to stimulus onset.

When the stimulus–response mapping is known during stimulus presentation, single-unit recordings in behaving monkeys as well as EEG and magnetoencephalographic studies in humans show a propagation of the evidence accumulation variable in the motor structures that prepare the response, similar to FR tasks. Importantly, ramping effector-selective motor preparation signals appear to plateau during the delay period before the RS (de Lafuente et al., 2015; de Lange et al., 2013; Donner et al., 2009; Horwitz & Newsome, 1999; Kiani et al., 2008; Rao et al., 2012; Rogge et al., 2022; Roitman & Shadlen, 2002; Shadlen & Newsome, 2001; Twomey et al., 2016). These findings suggest that a representation of the selected response is maintained at the motor preparation level, in the form of sustained activity that corresponds to the level of cumulative evidence. More generally, they suggest that evidence accumulation and working memory can be underpinned by similar cortical mechanisms (Harvey et al., 2012; Wang, 2008; Wong & Wang, 2006).

An important question concerns the mechanism that governs the transition between evidence accumulation and sustained activity. One possibility is that subjects accumulate all available evidence. A behavioral modeling study in humans provided strong evidence against this assumption (Ratcliff, 2006). Subjects appear to stop

[3] An EMG burst constitutes a precursor to force production. The conversion of myoelectric activity into muscle force involves a series of electrochemical and mechanical processes that are irrelevant to the present work.

Figure 1

Illustration of Motor Preparation and Muscle Activation Dynamics From GCD and GCD_{RS} Models

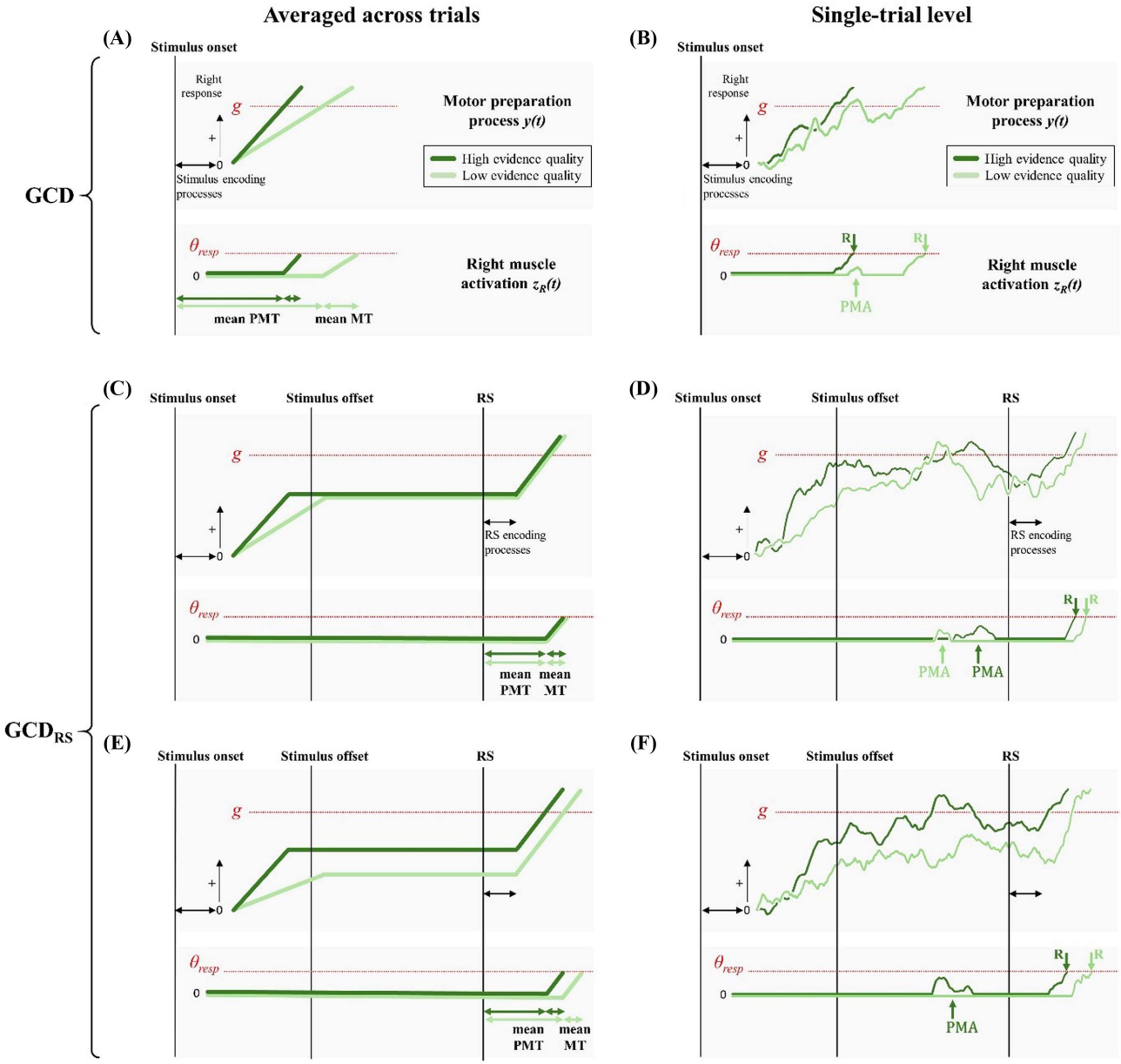

Note. The first row (Panels A–B) illustrates GCD dynamics in a free response decision task involving high (dark green) and low (light green) evidence quality conditions. The second and third rows (Panels C–F) illustrate GCD_{RS} dynamics in a response signal (RS) variant of the task involving a delay between stimulus offset and RS onset, and foreknowledge of the stimulus–response mapping. The first column (Panels A, C, and E) shows predicted motor preparation and muscle activation trajectories averaged across a large number of trials (i.e., the expected value). The second column (Panels B, D, and F) shows predicted motor preparation and muscle activation trajectories at the single-trial level. The contents of each panel are as follows. (A) According to GCD, the evidence accumulation variable continuously flows to motor preparation brain areas, and is subjected to gating inhibition (parameter g) before activating muscle fibers. The response occurs when muscle activation reaches a threshold level of activation (parameter θ_{resp}, referred to as response threshold). The lower accumulation rate for the low evidence quality condition produces an increase in both the mean premotor time (PMT, from stimulus onset to the onset of muscle activation) and the mean motor time (MT, from the onset of muscle activation to the response). (B) At the single-trial level, moment-by-moment internal noise produces random fluctuations in the motor preparation trajectory, and variability in the latency at which the response (R) occurs. GCD predicts a partial muscle activation (PMA) when the motor preparation trajectory temporarily exceeds the level of gating inhibition g, but the corresponding muscle activation does not reach the response threshold θ_{resp} (see light green trajectories). PMA are more likely to occur in the EMG channel associated with the response than in the opposite channel. Moreover, PMA are more likely to occur in the EMG channel associated with the response when the quality of evidence is low, due to the decrease in the signal-to-noise ratio of the motor preparation variable. (C) In the RS variant of the task, GCD_{RS} also assumes that the evidence accumulation variable continuously flows to motor preparation brain areas during stimulus presentation, but the level of gating

(figure continues)

accumulating evidence when the decision process reaches a threshold, similar to FR tasks. This study also showed that a perfect accumulation model (with no leakage in the accumulator memory) provided a better fit performance than a leaky accumulation variant, though differences in model selection statistics were small. The maintenance of the choice in working memory until the RS was not modeled. Monkeys also seem to use some kind of bounded perfect accumulation, as late samples of stimulus information have no effect on performance, unlike early samples (Kiani et al., 2008).

An apparent challenge for the bounded accumulation hypothesis concerns the modulation of sustained effector-specific motor preparation activities by the quality of evidence. Specifically, the average level of sustained activity during the delay period before the RS decreases as the quality of evidence decreases (de Lafuente et al., 2015; Kiani et al., 2008; Rao et al., 2012; Roitman & Shadlen, 2002; Shadlen & Newsome, 2001). The mechanism underlying this effect is unclear. It could result from a short post-threshold evidence accumulation period caused by a delay introduced by the (unknown) neural mechanism that compares activity to the threshold (Mazurek et al., 2003), or from a threshold that decreases as processing time increases due to the attentional cost of acquiring new samples of evidence (Cisek et al., 2009; Ditterich, 2006a, 2006b; Drugowitsch et al., 2012; Thura et al., 2012). Another possibility is that a proportion of evidence accumulation trajectories do not reach the threshold before transitioning to sustained activity, due to insufficient evidence in the processing pipeline. This proportion may increase when the quality of evidence decreases, especially when stimulus duration (or latency between stimulus onset and RS onset) is short (Ratcliff, 2006).

A few studies have examined behavioral performance and brain activity when the stimulus–response mapping is not known during stimulus presentation and is instead provided by the RS (or slightly before). As expected, effector-selective motor preparation activities are silent prior to the delivery of the stimulus–response mapping (Bennur & Gold, 2011; Gold & Shadlen, 2003; Shushruth et al., 2022; Twomey et al., 2016). In monkeys, two different processing strategies have been identified. One single-unit study showed ramping electrical signals during stimulus presentation followed by persistent activity that reflected the selected stimulus category (Bennur & Gold, 2011). Another single-unit study in monkeys failed to replicate these findings. Monkeys stored samples of evidence in working memory, and performed the decision only when the stimulus–response mapping was provided by the RS, through accumulation of evidence from memory (Shushruth et al., 2022).[4] Their behavioral performance was thus very close to that observed in FR tasks. The reason for discrepancies in processing strategy may be related to the training history of the monkeys (Shushruth et al., 2022). To our knowledge, only one study in humans has evaluated decision-related activities when the stimulus–response mapping is provided by the RS (Twomey et al., 2016). Centroparietal EEG signals showed ramping dynamics during stimulus presentation, the slope of which scaled with sensory evidence. This result indicates that subjects categorized the stimulus. Interestingly, centroparietal EEG signals did not plateau during the delay period before the RS and instead decayed back to baseline. The brain may have maintained the selected stimulus category elsewhere or may have used another neural mechanism for this short-term maintenance (e.g., short-term synaptic plasticity;[5] Masse et al., 2020).

Extending GCD to Delayed Decision Reports

Our literature review suggests that GCD can be extended to RS tasks without major changes in information processing components. When the stimulus–response mapping is known during stimulus presentation, one simply needs to assume that (a) gating inhibition is increased before the RS to prevent muscle activation and (b) the motor preparation process $y(t)$ plateaus during the delay period, consistent with neurophysiological studies. This raises the question of the mechanism that drives the muscles to the response threshold θ_{resp} after the RS. A decrease in gating inhibition is plausible, but it cannot produce the kind of ramping signals observed at the muscle activation level. To solve this problem, we first note that the detection of the RS corresponds to a one-choice RT task, which has been successfully modeled by a one-boundary evidence accumulation process (Ratcliff & Van Dongen, 2011; Smith, 1995). In line with this modeling work, we assume that subjects sample and accumulate evidence from the RS. This simple mechanism explains both RS detection and muscle activation. Specifically, the level of sustained activity of $y(t)$ at RS onset constitutes the starting point for a second phase of evidence

[4] Due to working memory capacity limitations, monkeys are unlikely to store the full stream of evidence from the stimulus. Using computer simulations, Shushruth et al. (2022) showed that the accumulation of a few samples of evidence can provide a reasonable approximation of psychometric functions obtained when integrating the full stream of evidence.

[5] The idea behind short-term synaptic plasticity is that synaptic connections are dynamically modulated in response to neuronal activity, allowing information to be stored in short-term memory without the need for sustained activity.

Figure 1 Note (continued). inhibition g increases to prevent muscle activation. During the delay, the representation of the selected response is maintained at the motor preparation level, in the form of sustained activity that corresponds to the level of cumulative evidence. When the RS is presented, subjects sample and accumulate evidence from it to drive muscles to the response threshold θ_{resp}. Gating inhibition may decrease to facilitate response production, but this adjustment does not have any impact on model predictions. If the average level of sustained activity during the delay is not modulated by the quality of evidence, as illustrated, GCD_{RS} predicts no effect of the quality of evidence on mean PMT (from RS onset to the onset of muscle activation) and mean MT (from the onset of muscle activation to the response). (D) At the single-trial level, the sustained motor preparation activity during the delay is not completely flat, due to moment-by-moment internal noise. Random fluctuations can cause PMA, as shown by the light and dark green trajectories. The probability of occurrence of PMA during the delay depends on the separation between the average level of sustained motor preparation activity and gating inhibition. Consequently, PMA are more likely to occur during the delay in the EMG channel associated with the response than in the opposite channel. If the average level of sustained activity is not modulated by the quality of evidence, as assumed here, then the rate of PMA in the EMG channel associated with the response during the delay should not vary between low and high evidence quality conditions. (E) If the average level of sustained motor preparation activity during the delay decreases as the quality of evidence, as illustrated, then mean PMT should be slower in the low compared to the high evidence quality condition, but mean MT should not be modulated. At the single-trial level (Panel F), the rate of PMA in the EMG channel associated with the response during the delay should be lower for the low compared to the high evidence quality condition, due to the larger separation between sustained motor preparation activity and gating inhibition on average. GCD = gated cascade diffusion model; GCD_{RS} = extension of the gated cascade diffusion model for response signal tasks. See the online article for the color version of this figure.

accumulation, where the evidence is sampled from the RS.[6] The sign of the accumulation rate is identical to the sign of the sustained activity, and its magnitude is determined by properties of the RS (see Figure 1C and 1E). To avoid confusion, we refer to the accumulation rate for the first phase (during stimulus presentation) as parameter v, and to the accumulation rate for the second phase (after the RS) as parameter w. If the stimulus–response mapping is delivered by the RS, the motor preparation variable $y(t)$ remains silent until the presentation of the RS, consistent with neurophysiological studies. The second phase of evidence accumulation driven by the RS thus starts at 0, and we assume that the sign of w is determined by the sign of cumulative evidence at the stimulus categorization level. We refer to this extended GCD for RS tasks as GCD_{RS}.

We conducted three experiments to test general predictions from GCD_{RS}. Each of these experiments used a RS variant of the random dot motion task. In the original FR variant of this task, subjects are presented with a field of moving dots, and are instructed to press one of two buttons (or produce a saccade toward one of two targets) as a function of the net direction of the dots. Decision difficulty is typically manipulated by varying motion coherence, defined as the proportion of dots moving in the target direction, the other dots moving randomly. The lower the coherence, the higher the difficulty of the decision. This task allows researchers to study the formation of decision and motor commands over a relatively long period of time, as it requires an integration of sensory evidence in time and space. In addition, manipulations of motion coherence typically produce larger modulations of mean RT compared to other perceptual manipulations. These properties make the random dot motion task particularly appropriate to test continuous flow models (Dendauw et al., 2024; Donner et al., 2009; Kelly & O'Connell, 2013; Roitman & Shadlen, 2002; Servant et al., 2021), and their extension to delayed decision reports in the context of the present work.

Each RS variant of the random dot motion task incorporated a short delay (minimum 3 s) between stimulus offset and RS onset. This delay allowed us to (a) evaluate processing characteristics associated with the short-term maintenance of information; (b) better characterize the articulation between decision-making, memory, and motor systems; and (c) prevent any strategical attempt to postpone the treatment of the stimulus (which could occur if the stimulus is presented until the RS or the response; e.g., Coallier & Kalaska, 2014; Twomey et al., 2016). In Experiments 1 and 2, the stimulus–response mapping was known before stimulus presentation. Experiment 1 manipulated the duration of the delay (3 vs. 5 vs. 7 s), and used a constant stimulus duration (2 s). Experiment 2 manipulated stimulus duration (0.3 vs. 1 vs. 2 s), and used a constant delay (3 s). Experiment 3 was similar to Experiment 1, except that the stimulus–response mapping was provided by the RS. GCD_{RS} makes predictions that will be presented in the introduction section of each experiment. These predictions will be tested using traditional behavioral measures extended with EMG measures of muscle activation.

Experiment 1

Experiment 1 was designed to test a first set of behavioral and EMG predictions from GCD_{RS} in a RS variant of the random dot motion task in which the stimulus–response mapping was known before stimulus presentation. In separate blocks of trials, participants also completed the original FR version of the task that served as a processing benchmark. They were instructed to press the left (right) button with their left (right) thumb, if the net direction of dots was leftward (rightward). The quality of evidence was manipulated by randomly varying motion coherence across three levels (2 vs. 11 vs. 40%) within blocks of trials. In FR blocks, stimuli were presented within a virtual circular aperture, and participants were instructed to respond as quickly and accurately as possible. Stimuli remained on the screen until the response. In RS blocks, the same stimuli were presented within a red circle during 2 s. The red circle remained on the screen during the delay period and its disappearance served as the RS. The duration of the delay was manipulated in separate blocks of trials (3 vs. 5 vs. 7 s; Figure 2A). The primary measures of interest were (a) response accuracy, (b) the rate of partial muscle activation, (c) the premotor time (PMT), (d) the slope of muscle activation, and (e) the motor time (MT: latency between the onset of muscle activation and the response).[7] In FR blocks, PMT was defined as the latency between stimulus onset and the onset of muscle activation. In RS blocks, PMT was defined as the latency between RS onset and the onset of muscle activation. In both tasks, the RT in each trial corresponded to the sum of PMT and MT.

Predictions From GCD in FR Blocks

Predictions from GCD in FR blocks have been derived and validated in previous work, in the context of a similar random dot motion task featuring a larger range of motion coherences (Dendauw et al., 2024; Servant et al., 2021). Specifically, accuracy should decrease as motion coherence decreases. Moreover, mean PMT, mean MT, and the rate of partial muscle activation in the EMG channel associated with the response should increase as motion coherence decreases. These predictions result from the decrease in the accumulation rate of the motor preparation process as motion coherence decreases (Panels A and B of Figure 1). The data from FR blocks will thus serve as a replication of these findings, as well as a processing benchmark for RS blocks.

Predictions From GCD_{RS} in RS Blocks

For the sake of clarity, GCD_{RS} predictions are presented below for each dependent variable separately.

Response Accuracy

The motion coherence manipulation in RS blocks should modulate the accumulation rate v of the motor preparation process during stimulus presentation. Response accuracy should thus decrease as motion coherence decreases. The comparison of accuracy performance between RS and FR blocks will be

[6] Evidence from the RS may be accumulated by both the stimulus categorization process $x(t)$ and the motor preparation process $y(t)$ through continuous flow. Alternatively, evidence from the RS might be directly accumulated at the motor preparation level through a direct processing route. These alternative hypotheses will not be further discussed, as they do not have any impact on model predictions in the context of the present work.

[7] In the context of the present work, the expression "slope of muscle activation" always refers to the slope of muscle activation leading to the response (not partial muscle activations). Similarly, PMT and MT are always defined with respect to the onset of muscle activation leading to the response.

Figure 2

Empirical Design and Results of Experiment 1

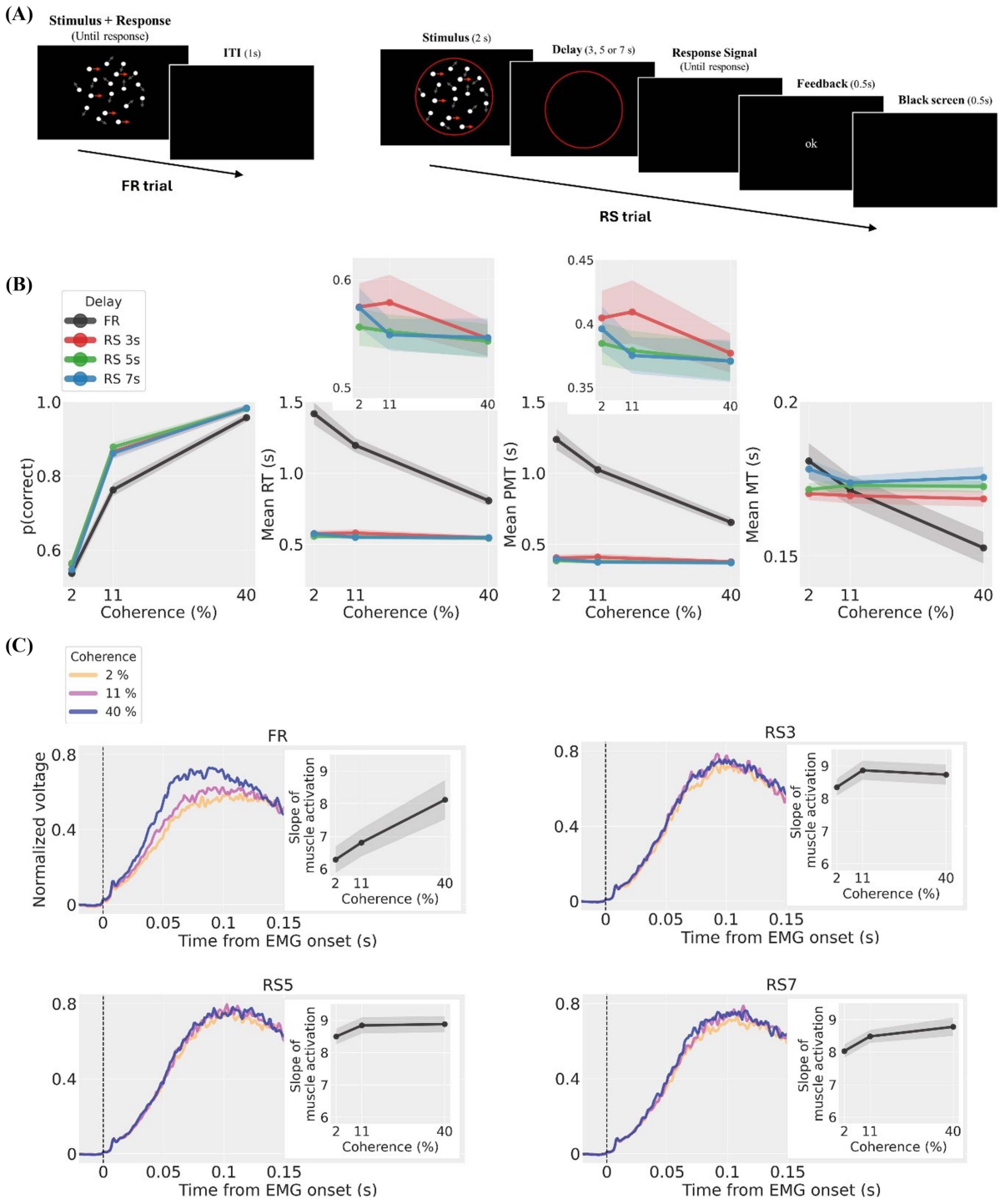

Note. (A) Trial structure in FR (left panel) and RS (right panel) blocks. See text for details. (B) Proportion of correct responses, mean RT, mean PMT, and mean MT for each condition averaged across subjects. Insets provide a zoom on data from RS blocks. (C) Muscle activation leading to the response for each condition averaged across subjects. EMG signals are time-locked to the onset of muscle activation, and are normalized with respect to the peak amplitude (detected for each subject on the response-locked EMG signal averaged across all conditions, in the 150 ms window before the response). Insets display the average slope of muscle activation for each condition, computed using linear regression in the 100 ms window after muscle activation onset. Shaded areas represent ±1 within-subjects standard error of the mean. FR = free response; RS = response signal; ITI = intertrial interval; RT = reaction time; PMT = premotor time; MT = motor time; EMG = electromyography. See the online article for the color version of this figure.

informative with respect to the amount of evidence used to inform the choice. For instance, a higher accuracy for RS than FR blocks would suggest that subjects sampled and accumulated more evidence from the stimulus on average in the former.

Slope of Muscle Activation and Mean MT

Since the activation of the muscle leading to the response in RS blocks is driven by evidence sampled from the RS, it should not vary on average as a function of motion coherence. Thus, mean MT and the slope of muscle activation should not be modulated by motion coherence, contrary to FR blocks.

Mean PMT

Mean PMT in RS blocks should be much shorter compared to FR blocks, because it does not incorporate stimulus categorization and response selection latencies. The predicted effect of motion coherence on mean PMT in RS blocks is more complex, and depends on the mechanism that governs the transition between the first phase of evidence accumulation and sustained activity at the motor preparation level. Based on our literature review, two processing schemes can be dissociated. If motor preparation accumulation trajectories on every trial reach the same level of sustained activity, then the starting point of motor preparation for the second phase of evidence accumulation should be the same across motion coherence levels. Consequently, mean PMT should not be modulated by motion coherence (Figure 1C). On the other hand, if motor preparation accumulation trajectories reach a lower asymptotic level on average as the quality of evidence decreases, GCD_{RS} predicts an increase in mean PMT as motion coherence decreases, because the starting point for the second phase of evidence accumulation is located father away from the gate on average (Figure 1E).

Rate of Partial Muscle Activation During the Delay

Although GCD_{RS} predicts an increase in gating inhibition during the delay to prevent muscle activation, noisy fluctuations of the motor preparation variable at the single-trial level may sometimes exceed the gate (for illustrations, see Panels D and F of Figure 1). The probability of occurrence of this phenomenon increases as the motor preparation variable gets closer to the gate (and vice versa). Consequently, the rate of partial muscle activation during the delay should be higher in the EMG channel associated with the selected response than in the EMG channel associated with the nonselected response. If motion coherence does not modulate the asymptotic level of motor preparation during the delay, the rate of partial muscle activation in the EMG channel associated with the selected response should not be modulated by motion coherence (Figure 1D). Alternatively, if a decrease in motion coherence leads to a decrease in asymptotic motor preparation activity, then this rate should decrease as motion coherence decreases (Figure 1F).

In its raw form, GCD_{RS} does not predict any effect of the delay manipulation on performance. Additional processing assumptions may be necessary, depending on the expected impact of this manipulation on sustained motor preparation activity and subsequent processing of the RS. Our literature review does not show evidence for a leakage in the accumulator memory, and thus this factor can be reasonably disregarded. However, the delay manipulation is likely to induce a different temporal preparation for the occurrence of the RS. Temporal preparation can modulate behavioral performance in certain contexts, so it seems necessary to review the relevant literature and articulate the main findings with GCD_{RS}. When the time interval between a warning signal and a stimulus (termed "foreperiod") is manipulated in separate blocks of trials, mean RT to the stimulus increases as the foreperiod increases (Woodrow, 1914). This effect is classically explained by the accuracy of temporal estimation, which decreases as the foreperiod increases (Weber's law). Thus, preparation for the upcoming trial decreases as the foreperiod increases (Requin et al., 1991). Temporal preparation effects are known to modulate multiple information processing components along the sensorimotor hierarchy. During the foreperiod, temporal preparation is associated with an increase in cortical excitability as well as an increase in inhibition at the corticospinal level to prevent premature responding (Burle et al., 2010). During stimulus presentation, temporal preparation facilitates early (e.g., perception) as well as late (muscle activation) processing stages (for reviews, see Burle et al., 2010; Rolke & Ulrich, 2010). For instance, EMG studies have shown that both mean PMT and mean MT increase as the foreperiod (manipulated in separate blocks of trials) increases, with the latter being caused by a decrease in the slope of muscle activation (Hasbroucq et al., 1995; Tandonnet et al., 2003). These effects are presumably caused by modulations in the control of attention and are mostly observed in attention-demanding tasks (Correa et al., 2006; Rolke, 2008; Seibold et al., 2023). Modulations in attentional control as a function of the different delays may occur in the present experiment, but we do not expect them to have a significant impact on performance for two reasons. First, an increase in the level of preparation for the selected response during the delay would increase the risk of premature responding, and would require an additional increase in gating inhibition. Whether this phenomenon occurs or not, the distance between the motor preparation variable and the gate within GCD_{RS} would remain constant on average. Consequently, the rate of partial muscle activation during the delay should not vary with its duration. Second, RS processing is not demanding, so we do not expect modulations in the control of attention to affect the rate of evidence accumulation in Phase 2. Consequently, mean PMT, mean MT, and the slope of muscle activation should not be modulated by the duration of the delay.

Method

Transparency and Openness

In the sections below, we report how we determined our sample size, all data exclusions, all experimental manipulations, and all measures in the study. All data, analysis code (written in Python), and research materials are freely available at https://osf.io/vf95p/. This study was not preregistered.

Participants

Servant et al. (2021) used a sample size of 18 subjects. Motion coherence explained 60% of variations of mean MT ($\eta_p^2 = .6$) and 40% of variations of muscle activation slope ($\eta_p^2 = .4$). An important prediction of the present work concerns the interaction between task variant (FR vs. RS) and motion coherence on the slope of muscle

activation and mean MT. Specifically, a decrease in motion coherence should decrease the slope and increase mean MT in the FR variant only. Consequently, we ran a power analysis using the MorePower 6.0 software (Campbell & Thompson, 2012) to detect a significant interaction between task variant and coherence with 80% power at the $\alpha = .05$ level, given an effect size conservatively set at $\eta_p^2 = .1$. This analysis showed that 22 participants were necessary to achieve this goal.

Twenty-two subjects (three men, 19 women; $M_{age} = 21.4$; range = 20–24; no further demographics were collected aside from gender and age) participated in Experiment 1 in exchange for a 20 euros gift card. Participants were students from the University of Franche-Comté recruited through online advertisement. All participants were right-handed, had a normal or corrected-to-normal vision, and no history of motor/psychiatric/neurological disorders. They were unaware of the purpose of the experiment and gave their written consent to participate. This study was approved by the ethical committee for research of the university (Agreement No. CERUBFC-2022-01-18-002).

Apparatus

The experiment was conducted in a dimly lit room and was run on a PC running Windows 10, using the programming language Python and components of the PsychoPy toolbox v3.2.4 (Peirce et al., 2019). Stimuli were displayed on a 34.42 × 19.36 cm LCD monitor (resolution: 1,920 × 1,080; framerate: 60 Hz, distance from monitor: 75 cm). Responses were transmitted to the computer using two thermoplastic rubber hand-held buttons connected to a Black Box Toolkit module designed to ensure millisecond accuracy. The force required to press each button was approximately 8.83 *N*. This response system was similar to that used by Servant et al. (2021). To minimize artifactual motor activity and maximize comfort, subjects' hands were palm-down and rested on a supportive cushion placed on their laps.

Stimuli

Random dot stimuli in the FR task variant were similar to those used by Servant et al. (2021). White dots (0.05° diameter) were displayed in a virtual 11.78° circular aperture centered on a 26.29° × 14.79° black field. A white noise algorithm was used to control motion: From each frame to the next, a percentage p of dots was randomly selected to move in the signal direction (leftward vs. rightward), and the remaining dots were randomly relocated.[8] Parameter p, referred to as motion coherence, was manipulated across three levels (2 vs. 11 vs. 40%). Signal dots moved at a speed of 10.5°/s, and the average number of dots per frame was 71. The RS variant of the task used the same stimuli, except that the dots were presented within a red circle (line width: 0.15°).

Procedure

Participants completed 12 blocks of 96 trials. There were three FR blocks and nine RS blocks. Three RS blocks featured a 3-s delay between stimulus offset and RS onset (referred to as RS3 blocks), three RS blocks featured a 5-s delay (RS5), and three RS blocks featured a 7-s delay (RS7). Blocks were presented in a pseudo-random order, with three repetitions of a random ordering of the four block types. Blocks were separated by self-paced breaks. We also introduced self-paced breaks in the middle of each RS5 and RS7 block to alleviate fatigue, given increased block duration and attentional demands. Participants were instructed to identify motion direction (leftward vs. rightward) and communicate their response by pressing the corresponding left or right button with their left or right thumb. In FR blocks, they were instructed to respond as quickly and as accurately as possible upon stimulus presentation. In RS blocks, they were instructed to respond as quickly and as accurately as possible upon RS presentation.

In each block, trials were defined by a factorial combination of motion direction (leftward vs. rightward) and motion coherence (2 vs. 11 vs. 40%). Each trial type appeared the same number of times in a random order. Each trial in FR blocks started with the presentation of the stimulus. The stimulus remained on the screen until the response or until a 4-s RT deadline. Failure to respond by then resulted in a "Too slow! Please respond faster" message displayed for 2 s. The intertrial interval was 1 s. In RS blocks, each trial started with the presentation of the stimulus within the red circle. Stimulus duration was fixed at 2 s, and the red circle remained on the screen during the delay. The disappearance of the red circle served as the RS. Each response (correct or incorrect) made after the RS and within the 4-s RT deadline was followed by the message "ok" displayed in white for 0.5 s. Note that this message was not a feedback on accuracy; it simply notified the participant that the response had been recorded (participants were informed of this). The next trial started after a 0.5-s blank screen. Premature responses (before the RS) prompted a "Too fast! Please respond after the disappearance of the red circle" message, which was displayed for 2 s. If participants failed to respond within the 4-s RT deadline, the message "Too slow! Please respond faster" was displayed for 2 s. Both messages were followed by a 1-s blank screen. The time course of each trial in FR and RS blocks is illustrated in Figure 2A. Participants first completed two blocks of 18 practice trials (each of the six possible stimuli was presented three times in a random order) before the experiment to ensure they understood the task. The first practice block was FR, and the second practice block was RS3. A feedback on accuracy ("Correct" vs. "Incorrect") was provided after each response for 1 s. Practice trials were discarded from analyses.

EMG Recording and Signal Processing

The EMG activity of a group of muscles (the *flexor pollicis brevis* in particular, involved in the flexion of the thumb at both carpo-metacarpal and metacarpophalangeal joints) was recorded using two active Ag/Cl electrodes fixed 1 cm apart on the skin of the thenar eminence of each hand. Electrodes were connected to a Biosemi ActiveTwo Mk2 biopotential measurement system (sampling frequency = 1,024 Hz). After data acquisition, the difference in voltage between each pair of electrodes was computed. Left and right bipolar EMG signals were then submitted to a 10-Hz high-pass Butterworth filter (3rd order) to remove slow drifts not related to EMG activity, rectified (i.e., we computed the absolute value of each voltage data

[8] This algorithm can be reproduced using the visual.DotStim() function of the PsychoPy toolbox and the following parameters: signalDots='different', noiseDots='position', dotLife = −1. Dots going off the edge of the stimulus were replaced randomly in the stimulus field. There was no limit to the number of frames that each dot could live for.

point), and segmented from −0.3 to 13 s relative to stimulus onset. We used the three-step procedure described in Servant et al. (2021) to detect EMG onsets, using more conservative parameters to increase the reliability of EMG onset detection in the presence of background noise (Appendix B). In a small proportion of trials, the amount of background noise was too large to detect EMG onsets, and these trials were discarded from analyses ($M = 0.33\%$ of FR trials, range 0%–1.74%; $M = 0.32\%$ of RS trials, range 0%–2.43%).

Data Analyses

Trials with anticipations (RTs < 200 ms; 0.02% of FR trials, 0.24% of RS trials), premature responses (1.46% of RS trials), or in which participants failed to respond within the 4-s RT deadline (0.55% of FR trials, 0.18% of RS trials) were excluded from analyses. Statistical analyses were conducted using the JASP software (v.0.16.4). The data were analyzed using both frequentist and Bayesian repeated-measures analyses of variance (ANOVAs) with block type (FR vs. RS3 vs. RS5 vs. RS7) and motion coherence (2 vs. 11 vs. 40%) as factors. Chronometric analyses were conducted on all trials (correct and incorrect), though similar findings were obtained when considering correct trials only. For the frequentist analyses, the significance level was set to .05. The assumption of sphericity was assessed using Mauchly's test, and the Greenhouse–Geisser correction was applied when sphericity was violated.[9] We report a partial η^2 statistic η_p^2 as a measure of effect size. For the Bayesian analyses, we report inclusion Bayes Factors (BF_{incl}) across matched models, which reflect the evidence for models including a particular effect (H_1) compared to equivalent models without that effect (H_0). Interpretations of BF_{incl} followed standard guidelines in the field (>100: decisive evidence for H_1; 30–100: very strong evidence for H_1; 10–30: strong evidence for H_1; 3–10: substantial evidence for H_1; 1–3: anecdotal evidence for H_1; 1: no evidence; and vice versa for H_0).

Results

The statistical results presented below are summarized in Table C1.

Response Accuracy

The proportion of correct responses in each condition averaged across subjects is presented in Figure 2B. An ANOVA with block type (FR vs. RS3 vs. RS5 vs. RS7) and motion coherence (2 vs. 11 vs. 40%) showed an interaction between the two factors, $F(3.82, 80.28) = 8.02$, $p < .001$, $\eta_p^2 = .28$, $BF_{incl} = 1.84 \times 10^5$ (decisive evidence for H_1). Response accuracy decreased as motion coherence decreased in both FR and RS blocks, consistent with predictions from GCD and GCD_{RS}. Response accuracy was also higher in RS than FR blocks, particularly in the 11% coherence condition. Subjects thus sampled and accumulated more evidence from the stimulus on average in RS than FR blocks. This effect was more pronounced in the intermediate coherence condition, likely due to floor and ceiling effects in the 2% and 40% coherence conditions, respectively.

To specifically evaluate the effect of the delay manipulation in RS blocks, we computed an ANOVA on the proportion of correct responses in RS blocks using delay (3 vs. 5 vs. 7 s) and motion coherence (2 vs. 11 vs. 40%) as factors. The delay manipulation did not modulate response accuracy, $F(2, 42) = 1.17$, $p = .32$, $BF_{incl} = 0.19$ (substantial evidence for H_0), and there was no interaction effect, $F(2.79, 58.48) < 1$, $BF_{incl} = 0.096$ (strong evidence for H_0).

Slope of Muscle Activation and Mean MT

Mean MT and the slope of muscle activation (estimated using linear regression in the 100-ms window from the onset of muscle activation to the peak amplitude) in each condition averaged across subjects are presented in Figure 2B and 2C, respectively. We first computed an ANOVA on mean MT with block type (FR vs. RS3 vs. RS5 vs. RS7) and motion coherence (2 vs. 11 vs. 40%) as factors. This analysis, which was the main target of our power analysis, revealed the predicted interaction between the two factors, $F(2.57, 54.06) = 18.80$, $p < .001$, $\eta_p^2 = .47$, $BF_{incl} = 2.29 \times 10^{14}$ (decisive evidence for H_1). Mean MT increased as motion coherence decreased in FR blocks only. This conclusion was backed up by an additional ANOVA on mean MT in RS blocks with coherence (2 vs. 11 vs. 40%) and delay (3 vs. 5 vs. 7 s) as factors. The analysis showed no effect of coherence, $F(2, 42) < 1$, $BF_{incl} = 0.14$ (substantial evidence for H_0), and no interaction between the two factors, $F(2.87, 60.17) = 1.86$, $p = .15$, $BF_{incl} = 0.54$ (anecdotal evidence for H_0).

We next performed the same analyses on the more sensitive slope of muscle activation. The first ANOVA with block type (FR vs. RS3 vs. RS5 vs. RS7) and motion coherence (2 vs. 11 vs. 40%) showed an interaction between the two factors, $F(3.31, 69.57) = 4.63$, $p = .004$, $\eta_p^2 = .18$, $BF_{incl} = 273$ (decisive evidence for H_1). Coherence primarily modulated the slope of muscle activation in FR blocks, consistent with the analysis performed on mean MT. However, this effect did not completely disappear in RS blocks. Consistent with this observation, the second ANOVA with coherence (2 vs. 11 vs. 40%) and delay (3 vs. 5 vs. 7 s) as factors showed an effect of motion coherence, $F(2, 42) = 8.55$, $p < .001$, $\eta_p^2 = .29$, $BF_{incl} = 11.10$ (strong evidence for H_1), no effect of delay, $F(2, 42) < 1$, $BF_{incl} = 0.28$ (substantial evidence for H_0), and no interaction between the two factors, $F(4, 84) < 1$, $BF_{incl} = 0.09$ (strong evidence for H_0). Thus, the slope of muscle activation in RS blocks decreased as motion coherence decreased, contrary to the prediction of GCD_{RS}, though the magnitude of this effect was very small, and obviously not sufficient to modulate mean MT.

Mean PMT

The mean PMT in each condition averaged across subjects is presented in Figure 2B. The ANOVA on mean PMT with block type (FR vs. RS3 vs. RS5 vs. RS7) and motion coherence (2 vs. 11 vs. 40%) as factors showed an interaction, $F(1.48, 31.06) = 53.74$, $p < .001$, $\eta_p^2 = .72$, $BF_{incl} = 2.54 \times 10^{34}$ (decisive evidence for H_1). Mean PMT was 586 ms faster in RS than FR blocks, and the effect of motion coherence was strongly reduced in the former. We next computed an ANOVA on mean PMT in RS blocks using delay (3 vs. 5 vs. 7 s) and motion coherence (2 vs. 11 vs. 40%) as factors. Mean

[9] A Bayesian repeated-measures ANOVA makes the same assumptions as a frequentist repeated-measures ANOVA. Violations of the sphericity assumption in the latter are known to substantially increase the Type I error rate. However, we do not know any procedure to correct for sphericity violations when conducting a Bayesian ANOVA. Consequently, BF_{incl} must be interpreted with caution when a violation of the sphericity assumption is apparent in the frequentist analyses (indicated by corrected degrees of freedom, which are decimal numbers).

PMT increased as motion coherence decreased, $F(2, 42) = 6.06$, $p = .005$, $\eta_p^2 = .22$, $BF_{incl} = 5.71$ (substantial evidence for H_1), though the amplitude of this effect was small (22 ms). The delay manipulation did not modulate mean PMT, $F(1.55, 32.46) = 1.40$, $p = .26$, $BF_{incl} = 0.35$ (anecdotal evidence for H_0), and there was no interaction effect, $F(4, 84) = 1.66$, $p = .17$, $BF_{incl} = 0.36$ (anecdotal evidence for H_0).

Rate of Partial Muscle Activation

The rate of partial muscle activation for each condition and EMG channel averaged across subjects is shown in Figure 3A. We first focused on the rate of partial muscle activation in the EMG channel associated with the response in FR blocks. An ANOVA with motion coherence as a factor showed that the rate increased as motion coherence decreased, $F(1.58, 33.21) = 36.50$, $p < .001$, $\eta_p^2 = .64$, $BF_{incl} = 1.45 \times 10^7$ (decisive evidence for H_1), consistent with GCD. We next analyzed the rate of partial muscle activation during the delay in RS blocks. An ANOVA with EMG channel (same as response vs. opposite) as a factor showed a higher rate of partial muscle activation in the channel associated with the response than in the opposite channel, $F(1, 21) = 13$, $p = .002$, $\eta_p^2 = .38$, $BF_{incl} = 28.11$ (strong evidence for H_1). This important finding is consistent with the hypothesis—core to GCD_{RS}—that a representation of the selected response is maintained in the form of sustained activity at the motor preparation level during the delay. We finally focused on the rate of partial muscle activation in the EMG channel associated with the response during the delay and computed an ANOVA with delay (3 vs. 5 vs. 7 s) and motion coherence (2 vs. 11 vs. 40%) as factors. Main effects of coherence and delay were not significant, $F(1.47, 30.95) = 1.77$, $p = .19$, $BF_{incl} = 0.35$ (anecdotal evidence for H_0) and $F(2, 42) = 1.80$, $p = .18$, $BF_{incl} = 0.53$ (anecdotal evidence for H_0), respectively, and the two factors did not interact, $F(4, 84) = 1.09$, $p = .37$, $BF_{incl} = 0.13$ (substantial evidence for H_0).

Discussion

Empirical findings obtained in the FR variant of the random dot motion task from Experiment 1 fully replicate those reported by Servant et al. (2021), and provide additional evidence for the GCD model framework. Empirical findings obtained in the RS variant are globally in line with GCD_{RS}. Specifically, mean PMT was 586 ms faster in RS than FR blocks, consistent with the hypothesis that subjects maintained a representation of the selected response at the motor preparation level during the delay period. Additional evidence for this assumption comes from the analysis of the partial muscle activation rate during the delay, which was higher in the EMG channel associated with the response than in the opposite channel.

Mean MT in RS blocks was not modulated by motion coherence, consistent with the hypothesis that the additional impulse necessary to overcome gating inhibition and activate muscles after the RS is predominantly driven by evidence sampled from the RS. However, the more sensitive analysis of the slope of muscle activation in RS blocks showed a reliable effect of motion coherence, with smaller slopes as motion coherence decreased. The size of this modulation was much smaller compared to that observed in FR blocks. Within GCD_{RS}, this unexpected finding suggests that the rate of evidence accumulation in Phase 2 (parameter w) slightly decreases as motion coherence decreases. Parameter w thus appears to be determined by two sources of evidence: evidence sampled from the RS and—to a much lesser extent—evidence from the motion stimulus retrieved from memory.

Mean PMT in RS blocks increased as motion coherence decreased, though the amplitude of this effect was small (22 ms). The modulation of parameter w mentioned above might have contributed to this finding. Another (not mutually exclusive) explanation concerns the processing scheme described in Figure 1E: A decrease in motion coherence might have decreased the average level of sustained motor preparation activity during the delay, thus increasing mean PMT. The lack of modulation of the partial muscle activation rate by motion coherence in the EMG channel associated with the response speaks against this hypothesis, as it suggests a constant level of sustained activity across coherence levels. However, this null effect should be interpreted with caution, because the evidence for H_0 was anecdotal. Moreover, the high level of gating inhibition and noise in the detection of partial muscle activations may have obscured subtle effects of coherence on sustained activity.

Although our analyses of partial muscle activations focused on the delay period in RS blocks for parsimony, the data in the two other periods (from stimulus onset to stimulus offset and from RS onset to the response), shown in Figure 3A, are also informative with respect to latent processing mechanisms. The rate of partial muscle activation in the EMG channel associated with the response clearly increased over the three periods. This phenomenon is fully consistent with GCD_{RS}: Gating inhibition is assumed to be at a similar level during stimulus presentation and the delay, but the motor preparation variable is at a lower level on average during stimulus presentation. After the RS, the motor preparation variable increases again (and gating inhibition possibly decreases). Thus, the probability of the motor preparation variable to overcome gating inhibition due to noise at the single-trial level increases over the three periods, consistent with observed data.

Finally, the manipulation of delay in RS blocks did not affect performance, consistent with our hypothesis. Although the evidence for this conclusion was often anecdotal, the EMG data did not show the classic markers of temporal preparation (Hasbroucq et al., 1995; Tandonnet et al., 2003). Therefore, a modulation of the memory delay in the context of the present experiment does not appear to require any additional processing assumption within GCD_{RS}.

Experiment 2

Experiment 2 was designed to test a second set of predictions from GCD_{RS}, when the duration of stimulus presentation is manipulated. Experiment 2 was thus similar to RS blocks from Experiment 1 except that (a) stimulus presentation duration was manipulated across three levels (0.3 vs. 1 vs. 2 s) within each block and (b) the delay between stimulus offset and RS onset was fixed at 3 s. No FR blocks were incorporated.

Predictions

The effect of the stimulus duration manipulation on the behavioral and EMG performance measures depends on its impact on the average level of sustained motor preparation activity during the delay. If evidence accumulation trajectories in Phase 1 reach the same threshold level before transitioning to sustained activity, regardless of stimulus duration, then the manipulation should not

Figure 3

Rate of PMA for Each Condition Averaged Across Subjects in Experiment 1 (Panel A), Experiment 2 (Panel B), and Experiment 3 (Panel C)

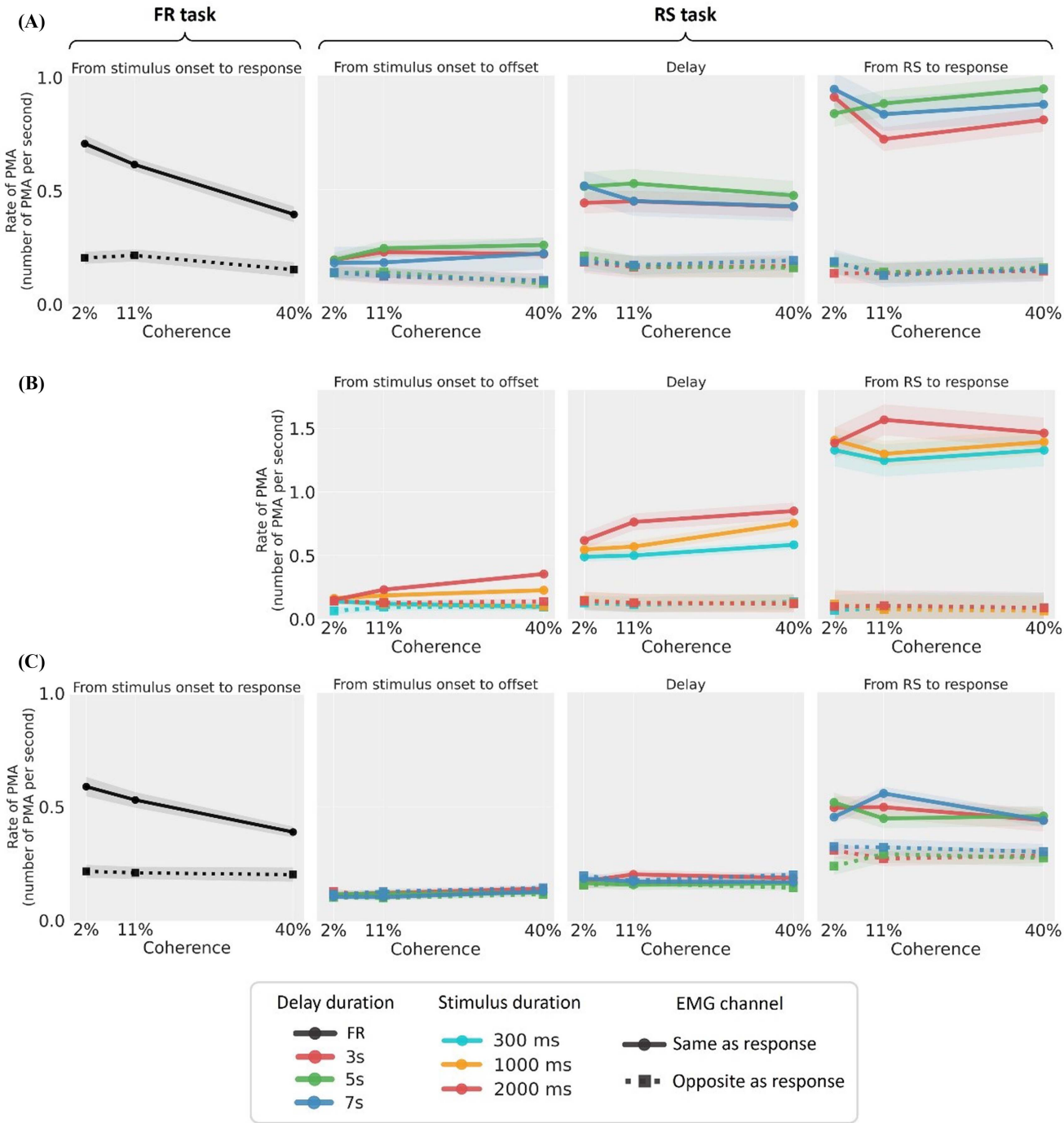

Note. PMA = partial muscle activation; FR = free response; RS = response signal; EMG = electromyography. See the online article for the color version of this figure.

have any effect on response accuracy, rate of partial muscle activation in the EMG channel associated with the response during the delay, and mean PMT. Conversely, if the average level of sustained motor preparation activity decreases with stimulus duration, possibly due to an increase in the proportion of evidence accumulation trajectories in Phase 1 that do not reach the threshold before transitioning to sustained activity, the rate of partial muscle activation in the EMG channel associated with the response

during the delay should decrease. Mean PMT should increase, because the starting point for the second phase of evidence accumulation is located father away from the gate on average. Finally, accuracy should decrease, because decisions based on nonterminated processes are less accurate than those based on terminated processes (Ratcliff, 2006). This modulation of accuracy may be most apparent in the intermediate (11%) coherence condition, due to potential floor and ceiling effects in the 2% and 40% coherence conditions, respectively. Any significant deviation from either set of predictions would call into question the architecture of the model.

Method

Participants

Twenty-two subjects took part in Experiment 2 (three men, 19 women; M_{age} = 21.04, range = 20–23; no further demographics were collected aside from gender and age) in exchange for a 20 euros gift card. None of the participants had taken part in Experiment 1. Participants were students from the University of Franche-Comté recruited through online advertisement. Criteria for inclusion in the study were similar to those used in Experiment 1. Participants gave written consent to participate. This study was approved by the ethical committee for research of the university (Agreement No. CERUBFC-2022-01-18-002).

Apparatus

The apparatus was identical to Experiment 1.

Stimuli

Stimuli were identical to Experiment 1.

Procedure

Participants completed 10 blocks of 90 trials, with self-paced breaks between blocks. Blocks were similar to RS blocks in Experiment 1, except that (a) the delay between the offset of the stimulus and the onset of the RS was fixed at 3 s, and (b) stimulus presentation duration was manipulated within each block. Each trial was thus defined by a factorial combination of motion direction (leftward vs. rightward), motion coherence (2 vs. 11 vs. 40%), and stimulus duration (0.3 vs. 1 vs. 2 s). Each trial type appeared the same number of times in a random order. The time course of each trial is illustrated in Figure 4A. Participants first completed a block of 18 practice trials (each stimulus type was presented once in a random order) before the experiment to ensure they understood the task. Practice trials were discarded from analyses.

EMG Recording and Signal Processing

EMG recording and signal processing were identical to Experiment 1 with one exception: signals were segmented from −0.3 s to 9 s relative to stimulus onset. The percentage of trials in which EMG onsets could not be detected due to a high level of background noise was small (M = 0.56%, range 0%–2.63%).

Data Analyses

Trials with anticipations (RTs < 200 ms; 0.39%), premature responses (0.04%), or in which participants failed to respond within the 4-s RT deadline (0.3%) were excluded from analyses. The data were analyzed using both frequentist and Bayesian repeated-measures ANOVAs, similar to Experiment 1.

Results

The statistical results presented below are summarized in Table C2.

Response Accuracy

The proportion of correct responses in each condition averaged across subjects is shown in Figure 4B. An ANOVA with motion coherence (2 vs. 11 vs. 40%) and stimulus duration (0.3 vs. 1 vs. 2 s) showed an interaction between the two factors, $F(3.72, 78.05) = 3.90$, $p = .006$, $\eta_p^2 = .16$, $BF_{incl} = 8.83$ (strong evidence for H_1). Accuracy decreased as motion coherence decreased. Accuracy was also lower in the 0.3 s compared to 1 s and 2 s stimulus duration conditions, and this effect was apparent in the 11% coherence condition only. Note, however, that accuracy did not differ between 1 s and 2 s stimulus duration conditions at the 11% coherence level (post hoc pairwise comparison corrected with Holm's procedure: $p = 1$), possibly due to a ceiling effect.

Slope of Muscle Activation and Mean MT

Mean MT and the slope of muscle activation (estimated using linear regression in the 100-ms window from the onset of muscle activation to the peak amplitude) in each condition averaged across subjects are presented in Figure 4B and 4C, respectively. An ANOVA computed on mean MT with motion coherence (2 vs. 11 vs. 40%) and stimulus duration (0.3 vs. 1 vs. 2 s) as factors showed no effect of motion coherence, $F(1.48, 31.16) = 2.57$, $p = .11$, though the Bayes factor could not distinguish between H_0 and H_1 ($BF_{incl} = 1.02$). The effect of stimulus duration and the interaction between the two factors were not significant, $F(2, 42) < 1$, $BF_{incl} = 0.15$ (substantial evidence for H_0) and $F(4, 84) < 1$, $BF_{incl} = 0.39$ (anecdotal evidence for H_0).

We next performed the same analysis on the slope of muscle activation. The ANOVA showed a reliable effect of coherence, $F(1.52, 31.88) = 5.35$, $p = .02$, $\eta_p^2 = .20$, $BF_{incl} = 5.17$ (substantial evidence for H_1). The slope decreased as motion coherence decreased, though the amplitude of this effect was small, similar to Experiment 1. Neither the effect of stimulus duration nor the interaction between the two factors were significant, $F(2, 42) < 1$, $BF_{incl} = 0.15$ (substantial evidence for H_0) and $F(4, 84) = 1.65$, $p = .17$, $BF_{incl} = 0.39$ (anecdotal evidence for H_0) respectively.

Mean PMT

The mean PMT in each condition averaged across subjects is presented in Figure 4B. The ANOVA on mean PMT with motion coherence (2 vs. 11 vs. 40%) and stimulus duration (0.3 vs. 1 vs. 2 s) as factors showed an effect of coherence, $F(1.16, 24.32) = 6.10$, $p = .02$, $\eta_p^2 = .23$, $BF_{incl} = 10.06$ (very strong evidence for H_1), an effect of stimulus duration, $F(2, 42) = 36.94$, $p < .001$, $\eta_p^2 = .64$, $BF_{incl} = 1.50 \times 10^7$ (decisive evidence for H_1), and no interaction between the two factors, $F(4, 84) < 1$, $BF_{incl} = 0.05$ (strong evidence for H_0).

Figure 4

Empirical Design and Results of Experiment 2

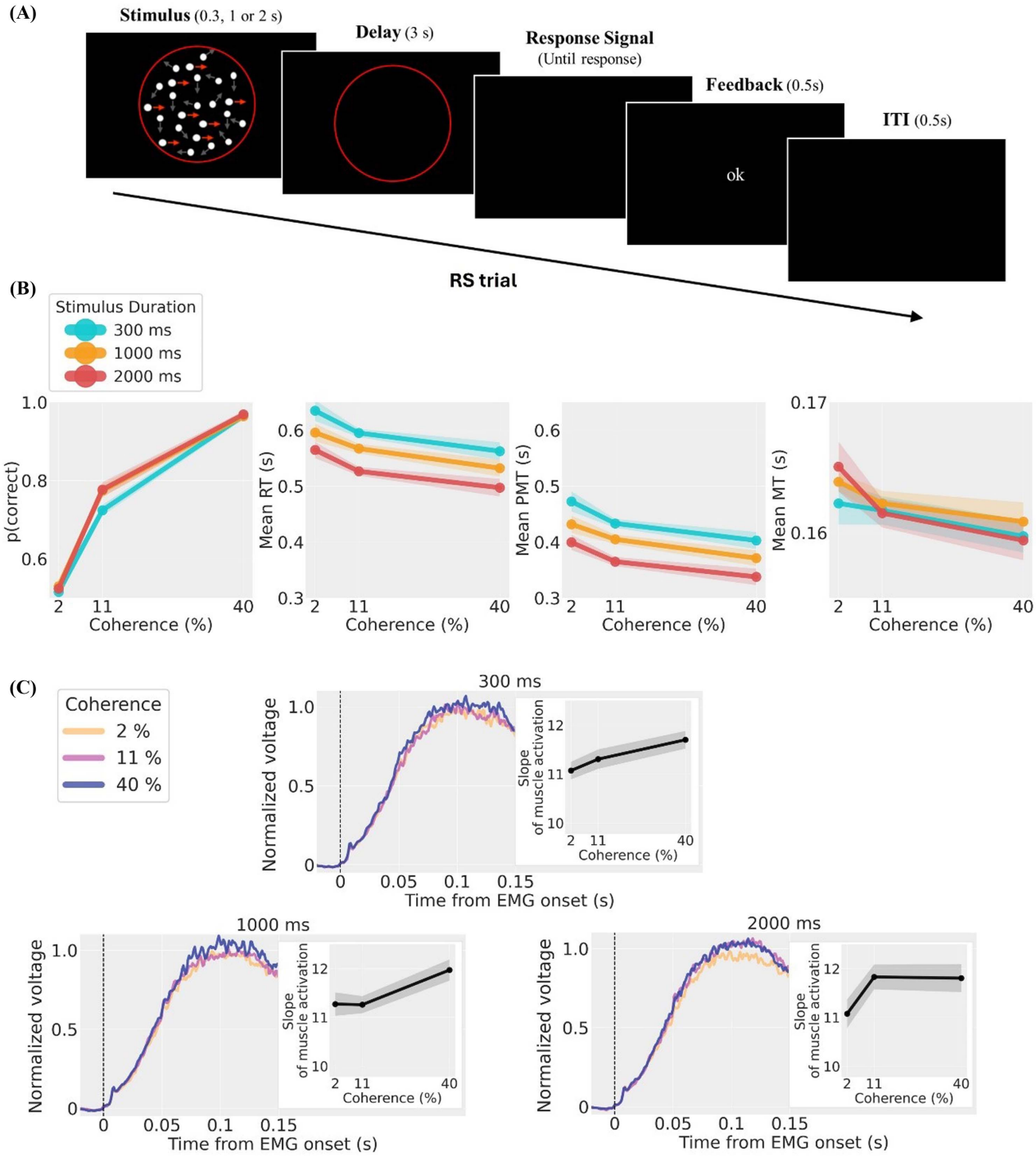

Note. (A) Structure of a trial, see text for details. (B) Proportion of correct responses, mean RT, mean PMT, and mean MT for each condition averaged across subjects. (C) Muscle activation leading to the response for each condition averaged across subjects. EMG signals are time-locked to the onset of muscle activation and are normalized with respect to the peak amplitude (detected for each subject on the response-locked EMG signal averaged across all conditions, in the 150 ms window before the response). Insets display the average slope of muscle activation for each condition, computed using linear regression in the 100 ms window after muscle activation onset. Shaded areas represent ±1 within-subjects standard error of the mean. RS = response signal; ITI = intertrial interval; RT = reaction time; PMT = premotor time; MT = motor time; EMG = electromyography. See the online article for the color version of this figure.

Mean PMT increased as motion coherence and stimulus duration decreased.

Rate of Partial Muscle Activation

The rate of partial muscle activation for each condition and EMG channel averaged across subjects is shown in Figure 3B. We first computed an ANOVA on this rate with EMG channel (same as response vs. opposite) as a factor. This analysis showed a higher rate of partial muscle activation in the channel associated with the response than in the opposite channel, $F(1, 21) = 14.89$, $p < .001$, $\eta_p^2 = .42$, $BF_{incl} = 156$ (decisive evidence for H_1). We next focused on the rate of partial muscle activation in the channel associated with the response, and computed an ANOVA with motion coherence (2 vs. 11 vs. 40%) and stimulus duration (0.3 vs. 1 vs. 2 s) as factors. This analysis showed main effects of motion coherence and stimulus duration, $F(1.19, 25.08) = 5.87$, $p = .02$, $\eta_p^2 = .22$, $BF_{incl} = 8.67$ (substantial evidence for H_1) and $F(1.22, 25.71) = 13.92$, $p < .001$, $\eta_p^2 = .40$, $BF_{incl} = 910$ (decisive evidence for H_1), respectively. The rate of partial muscle activation in the channel associated with the response decreased as motion coherence and stimulus duration decreased. The interaction between the two factors was not significant, $F(1.86, 39.04) = 2.25$, $p = .12$, $BF_{incl} = 0.70$ (anecdotal evidence for H_0).

Discussion

The manipulation of stimulus duration had several effects on performance. First, decreasing stimulus duration to 0.3-s decreased response accuracy in the intermediate (11%) motion coherence condition. Second, the rate of partial muscle activation in the EMG channel associated with the response during the delay decreased as stimulus duration decreased. Finally, mean PMT increased as stimulus duration decreased. These results are consistent with GCD_{RS}, and suggest that the average level of sustained motor preparation activity during the delay decreases as stimulus duration decreases.

Similar to Experiment 1, the slope of muscle activation decreased as motion coherence decreased, and the amplitude of this effect was too small to produce a reliable modulation of mean MT. These findings provide additional evidence for the hypothesis that the rate of evidence accumulation in Phase 2 within GCD_{RS} (parameter w) is determined by two sources of evidence: evidence sampled from the RS and—to a much lesser extent—evidence from the motion stimulus retrieved from memory. The motion coherence manipulation also modulated mean PMT. Specifically, mean PMT increased as coherence decreased, and the amplitude of this modulation was three times larger (66 ms) than that observed in Experiment 1 (22 ms). The modulation of parameter w could have contributed to this effect, but the analysis of the partial muscle activation rate in the EMG channel associated with the response indicates an additional cause. We found that this rate decreased as motion coherence decreased, suggesting that the average level of sustained motor preparation activity during the delay decreased as coherence decreased, thus increasing mean PMT.[10]

Experiment 3

Experiment 3 was designed to test a third set of predictions from GCD_{RS}, when the stimulus–response mapping is not known during stimulus presentation, but is instead delivered by the RS. Experiment 3 was similar to Experiment 1, but comprised two important differences. First, motion direction was either upward or downward (coherence levels were identical to the previous experiments). This feature was introduced to avoid a potential conflict between motion direction and response side. Second, the RS was either the letter M or S. Half of the subjects were instructed to associate upward and downward motion directions with left and right responses, respectively, if the RS was M (and vice versa for the letter S). The rule was reversed for the other half of subjects. FR blocks alternated with RS blocks (similar to Experiment 1) to ensure that the effects observed using leftward/rightward motion directions and left/right responses replicate when using upward/downward motion directions and left/right responses. The stimulus–response mapping for FR blocks was provided at the beginning of the experiment and alternated between participants.

Predictions

In line with empirical results reported by Twomey et al. (2016) in humans (see the general introduction section), we assume the following processing scheme in RS blocks. When the stimulus is presented, subjects perform a decision about its category (upward vs. downward), and store the representation of the chosen category in working memory during the delay. When the RS is presented, subjects combine and accumulate evidence from both the RS letter and the stimulus category representation to drive the muscles to the response threshold. Note that the number of processing steps involved in this activation function is greater than the simple scheme proposed for the previous experiments. Specifically, subjects must retrieve the stimulus–response mapping associated with the RS letter from memory and translate the stimulus category into a response accordingly. Consequently, mean PMT in RS blocks should be slower compared to Experiments 1 and 2, and the rate of partial muscle activation in the EMG channel associated with the response should be higher than in the opposite channel only after the RS. Based on findings from the previous experiments, we further assume that subjects incorporate a few samples of motion evidence retrieved from memory during the second phase of accumulation, so parameter w should slightly decrease as motion coherence decreases. This modulation may not be large enough to affect mean PMT and mean MT, but it should be detectable on the slope of muscle activation.

Finally, Experiment 3 incorporated the same delay manipulation as Experiment 1 in RS blocks (3 vs. 5 vs. 7 s, manipulated in separate blocks of trials). Since RS processing is considerably more challenging compared to Experiment 1, the decrease in attentional resources allocated to the RS as the delay increases should decrease the rate of evidence accumulation in Phase 2 within GCD_{RS}. Consequently, we predict an increase in mean PMT and mean MT as the delay increases, as well as a decrease in the slope of muscle activation.

[10] Note that the partial muscle activation data over the three periods (stimulus presentation, delay, and RS) replicate findings from Experiment 1. Specifically, the rate of partial muscle activation in the EMG channel associated with the response increased over the three periods, consistent with GCD_{RS} (see the Discussion section of Experiment 1).

Method

Participants

The sample size was increased to 24 subjects to accommodate our counterbalancing scheme (see below). Twenty-four subjects thus took part in Experiment 3 (three men, 21 women; $M_{age} = 21.04$, range = 20–23; no further demographics were collected aside from gender and age) in exchange for a 20 euros gift card. None of the participants had taken part in Experiments 1 and 2. Participants were students from the University of Franche-Comté recruited through online advertisement. Criteria for inclusion in the study were similar to those used in the previous experiments. Participants gave written consent to participate. This study was approved by the ethical committee for research of the university (Agreement No. CERUBFC-2022-01-18-002).

Apparatus

The apparatus was identical to Experiments 1 and 2.

Stimuli

Stimuli in FR and RS blocks were identical to those used in FR and RS blocks in Experiment 1, except that motion direction was either upward or downward. In addition, the RS was either the letter M or S (font: Consolas; 0.31° × 0.38°), presented at the center of the screen.

Procedure

Participants completed 12 blocks of 96 trials (three FR blocks, three RS3 blocks, three RS5 blocks, and three RS7 blocks). The number of trials per condition was thus identical to Experiment 1. We introduced self-paced breaks between blocks and in the middle of each RS5 and RS7 block to alleviate fatigue. Participants were instructed to identify motion direction (upward vs. downward) and communicate their response by pressing the corresponding button with their left or right thumb (Figure 5A). In FR blocks, half of the participants were instructed to press the left button if motion direction was upward and the right button if motion direction was downward. This mapping was reversed for the other half. With the exception of motion direction, the internal structure of each FR block was identical to Experiment 1. In RS blocks, half of the subjects were instructed to associate upward and downward motion directions with left and right responses, respectively, if the RS was the letter M (and vice versa if the RS was the letter S). The rule was reversed for the other half of subjects. In each RS block, trials were defined by a factorial combination of motion direction (upward vs. downward), motion coherence (2 vs. 11 vs. 40%), and RS (M vs. S). Each trial type appeared the same number of times in a random order. Other than that, the internal structure of RS blocks was identical to RS blocks in Experiment 1. The factorial combination of the stimulus–response mapping in FR blocks and the stimulus–response mapping in RS blocks resulted in four different combinations that were repeated six times (hence the 24 subjects). For each subject, FR and RS blocks were pseudorandomized using the same scheme as in Experiment 1. Participants first completed two blocks of practice trials to ensure they understood the task. The first block was FR and comprised 18 trials (each of the six stimulus types presented three times in a random order). The second block was RS3 and comprised 36 trials (each of the six stimulus types presented three times with each RS letter).

EMG Recording and Signal Processing

EMG recording and signal processing were identical to Experiment 1. The percentage of trials in which the EMG onset of the response could not be detected, due to a high level of noise was small ($M = 0.32\%$, range 0%–1.57%).

Data Analyses

Trials with anticipations (RTs < 200 ms; 0.01%), premature responses (0.2%), or in which participants failed to respond within the 4-s RT deadline (0.3%) were excluded from analyses. The data were analyzed with both frequentist and Bayesian repeated-measures ANOVAs, similar to previous experiments.

Results

The statistical results presented below are summarized in Table C3.

Response Accuracy

The proportion of correct responses in each condition averaged across subjects is presented in Figure 5B. An ANOVA with block type (FR vs. RS3 vs. RS5 vs. RS7) and motion coherence (2 vs. 11 vs. 40%) showed main effects of coherence and block type, $F(1.57, 36.17) = 434.04$, $p < .001$, $\eta_p^2 = .95$, $BF_{incl} = 4.52 \times 10^{27}$ (decisive evidence for H_1) and $F(1.56, 35.98) = 3.90$, $p = .04$, $\eta_p^2 = .15$, $BF_{incl} = 1.56$ (anecdotal evidence for H_1), respectively. Response accuracy decreased as coherence decreased and was slightly higher for RS than FR blocks. Although the amplitude of the block type effect was numerically larger in the 11% coherence condition, the interaction between the two factors was not significant, $F(3.19, 73.47) = 1.73$, $p = .17$, $BF_{incl} = 0.36$ (anecdotal evidence for H_0).

To specifically evaluate the effect of the delay manipulation in RS blocks, we computed an additional ANOVA on the proportion of correct responses in RS blocks with delay (3 vs. 5 vs. 7 s) and motion coherence (2 vs. 11 vs. 40%) as factors. The delay manipulation did not modulate response accuracy, $F(2, 46) < 1$, $BF_{incl} = 0.04$ (strong evidence for H_0), and there was no interaction effect, $F(2.80, 64.50) = 1$, $p = .40$, $BF_{incl} = 0.015$ (decisive evidence for H_0).

Slope of Muscle Activation and Mean MT

Mean MT and the slope of muscle activation (estimated using linear regression in the 70 ms window from the onset of muscle activation to the peak amplitude) in each condition averaged across subjects are presented in Figure 5B and 5C, respectively. An ANOVA on mean MT with block type (FR vs. RS3 vs. RS5 vs. RS7) and motion coherence (2 vs. 11 vs. 40%) showed an interaction between the two factors, $F(2.74, 62.96) = 9.35$, $p < .001$, $\eta_p^2 = .29$, $BF_{incl} = 3.94 \times 10^6$ (decisive evidence for H_1). Mean MT increased as motion coherence decreased, and the amplitude of this effect was larger in FR than RS blocks. A second ANOVA on mean MT data from RS blocks with coherence (2 vs. 11 vs. 40%) and delay (3 vs. 5 vs. 7 s) as factors showed reliable main effects of coherence and

Figure 5

Empirical Design and Results of Experiment 3

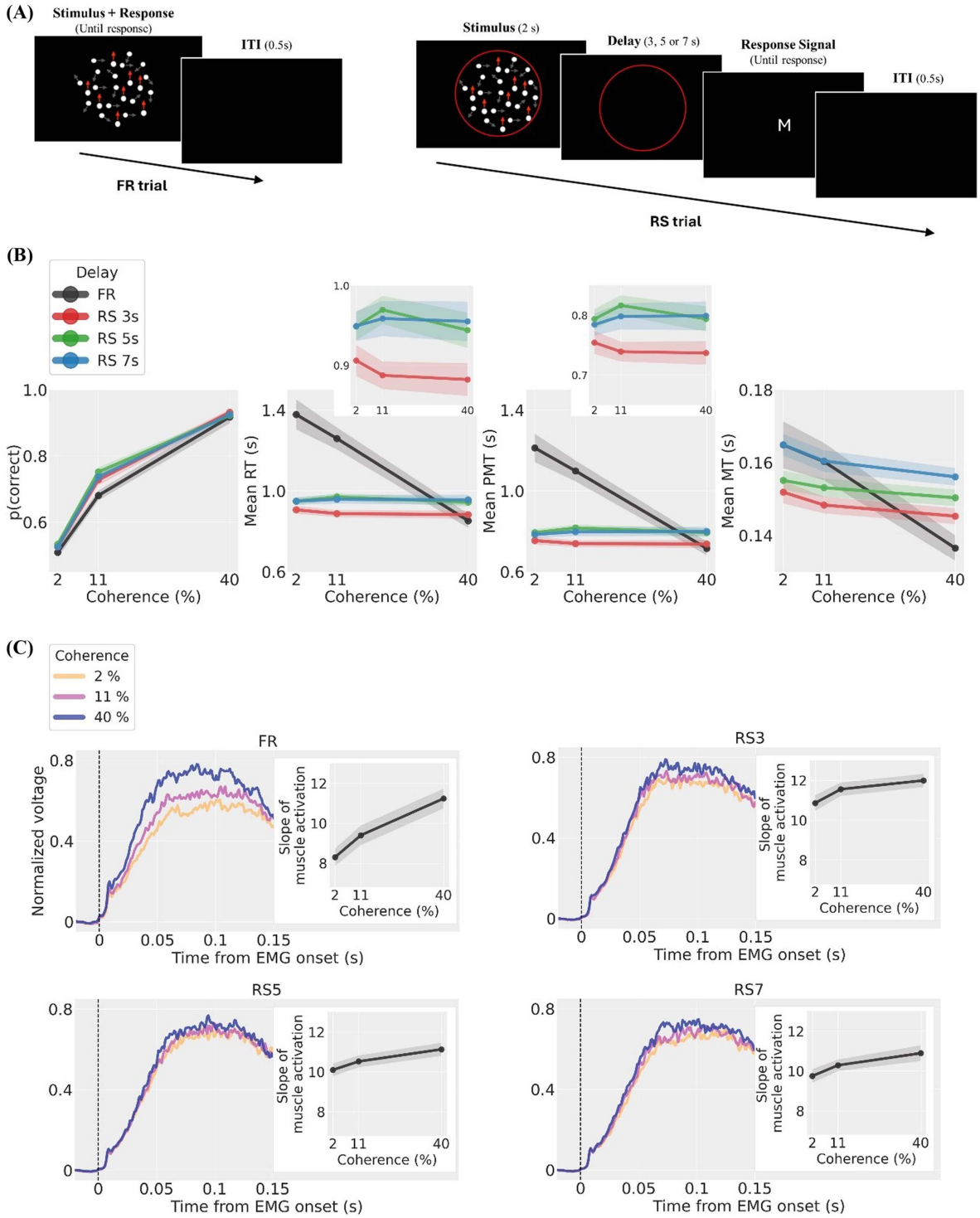

Note. (A) Trial structure in FR (left panel) and RS (right panel) blocks. See text for details. (B) Proportion of correct responses, mean RT, mean PMT, and mean MT for each condition averaged across subjects. Insets provide a zoom on data from RS blocks. (C) Muscle activation leading to the response for each condition averaged across subjects. EMG signals are time-locked to the onset of muscle activation and are normalized with respect to the peak amplitude (detected for each subject on the response-locked EMG signal averaged across all conditions, in the 150 ms window before the response). Insets display the average slope of muscle activation for each condition, computed using linear regression in the 70 ms window after muscle activation onset. Shaded areas represent ±1 within-subjects standard error of the mean. FR = free response; RS = response signal; ITI = intertrial interval; RT = reaction time; PMT = premotor time; MT = motor time; EMG = electromyography. See the online article for the color version of this figure.

delay, $F(2, 46) = 11.44$, $p < .001$, $\eta_p^2 = .33$, $BF_{incl} = 135$ (decisive evidence for H_1) and $F(2, 46) = 8.98$, $p < .001$, $\eta_p^2 = .28$, $BF_{incl} = 55$ (very strong evidence for H_1), respectively, but no interaction between the two factors, $F(2.67, 61.51) < 1$, $BF_{incl} = 0.06$ (strong evidence for H_0). Mean MT increased as motion coherence decreased, and increased as the delay increased.

We next computed an ANOVA on the slope data with block type (FR vs. RS3 vs. RS5 vs. RS7) and motion coherence (2 vs. 11 vs. 40%) as factors. This analysis showed an interaction between the two factors, $F(6, 138) = 7.36$, $p < .001$, $\eta_p^2 = .24$, $BF_{incl} = 8.91 \times 10^4$ (decisive evidence for H_1). The slope of muscle activation decreased as coherence decreased, and the amplitude of this effect was larger in FR than RS blocks. An additional ANOVA on the slope data from RS blocks with coherence (2 vs. 11 vs. 40%) and delay (3 vs. 5 vs. 7 s) as factors showed reliable main effects of coherence and delay, $F(2, 46) = 13.83$, $p < .001$, $\eta_p^2 = .38$, $BF_{incl} = 145$ (decisive evidence for H_1) and $F(1.56, 35.88) = 8.72$, $p = .002$, $\eta_p^2 = .27$, $BF_{incl} = 57$ (very strong evidence for H_1), respectively, but no interaction between the two factors, $F(4, 92) < 1$, $BF_{incl} = 0.05$ (strong evidence for H_0). The slope of muscle activation decreased as motion coherence decreased. It also decreased as the delay increased.

Mean PMT

The mean PMT in each condition averaged across subjects is presented in Figure 5B. An ANOVA on mean PMT with block type (FR vs. RS3 vs. RS5 vs. RS7) and motion coherence (2 vs. 11 vs. 40%) revealed an interaction between the two factors, $F(1.48, 33.93) = 39.41$, $p < .001$, $\eta_p^2 = .63$, $BF_{incl} = 4.34 \times 10^{26}$ (decisive evidence for H_1). Mean PMT increased as motion coherence decreased in FR blocks only. This was confirmed by a second ANOVA computed on mean PMT in RS blocks with coherence (2 vs. 11 vs. 40%) and delay (3 vs. 5 vs. 7 s) as factors. The main effect of coherence was not significant, $F(1.34, 30.82) < 1$, $BF_{incl} = 0.13$ (substantial evidence for H_0), and there was no interaction between coherence and delay, $F(4, 92) = 1.55$, $p = .19$, $BF_{incl} = 0.26$ (substantial evidence for H_0). The effect of delay was significant, $F(2, 46) = 7.99$, $p = .001$, $\eta_p^2 = .26$, $BF_{incl} = 37$ (very strong evidence for H_1), reflecting a faster mean PMT in the 3 s compared to the 5 s and 7 s delay conditions.

Rate of Partial Muscle Activation

The rate of partial muscle activation for each condition and EMG channel averaged across subjects is shown in Figure 3C. We first analyzed the rate of partial muscle activation in the EMG channel associated with the response in FR blocks. An ANOVA with motion coherence as a factor showed that the rate increased as motion coherence decreased, $F(1.43, 32.78) = 21.89$, $p < .001$, $\eta_p^2 = .35$, $BF_{incl} = 5.98 \times 10^4$ (decisive evidence for H_1). We next focused on the rate of partial muscle activation in RS blocks. An ANOVA on this rate with EMG channel (same as response vs. opposite) and period (stimulus presentation vs. delay vs. post-RS) showed a significant interaction between the two factors, $F(1.04, 23.82) = 23.54$, $p < .001$, $\eta_p^2 = .51$, $BF_{incl} = 1.75 \times 10^6$ (decisive evidence for H_1). Analyses of simple effects for the channel factor showed a significant effect after the RS only (stimulus presentation: $p = .97$, $BF_{incl} = 0.28$ [substantial evidence for H_0]; delay: $p = .55$, $BF_{incl} = 0.33$ [substantial evidence for H_0]; RS: $p < .001$, $BF_{incl} = 269$ [decisive evidence for H_1]), reflecting a higher rate of partial muscle activation in the channel associated with the response compared to the opposite channel, consistent with our hypothesis.

Discussion

Empirical results in FR blocks replicate those observed in Experiment 1. Mean PMT and mean MT increased as motion coherence decreased, the latter being caused by a decrease in the slope of muscle activation. Moreover, the rate of partial muscle activation in the EMG channel associated with the response increased as coherence decreased. These findings demonstrate that the effects observed using leftward/rightward motion directions and left/right responses replicate when using upward/downward motion directions and left/right responses, consistent with GCD.

The data from RS blocks are generally consistent with our hypotheses. The rate of partial muscle activation was higher in the EMG channel associated with the response than in the opposite channel only after the RS, suggesting that subjects did not prepare a specific response during the delay. Accordingly, mean PMT in RS blocks was generally slower ($M = 780$ ms) compared to that observed in Experiment 2 ($M = 402$ ms) and Experiment 1 ($M = 385$ ms), due to the additional processing operations to translate the representation of the stimulus category into a response. Mean MT increased and the slope of muscle activation decreased as motion coherence decreased. Within GCD_{RS}, this finding suggests that subjects retrieved some samples of motion evidence from memory during the second phase of accumulation. Since mean PMT was not modulated by coherence, this retrieval process must have occurred after the accumulation variable had crossed the gate, perhaps as a final attempt to check the decision.

Finally, the mean PMT and mean MT data showed the typical markers of temporal preparation (Hasbroucq et al., 1995; Tandonnet et al., 2003), consistent with our hypothesis. Specifically, mean PMT and mean MT were faster in the 3 s compared to the longer delay conditions, and the slope of muscle activation was steeper. Within GCD_{RS}, these effects can be explained by a modulation of the rate of evidence accumulation in Phase 2, due to variations in temporal attention.

General Discussion

The aim of this work was to extend current continuous flow models of immediate decision reports to delayed decision reports occurring after a relatively short time period (up to 7 s). We proposed a simple extension of the GCD model framework, termed GCD_{RS}, based on empirical findings suggesting similar cortical mechanisms for decision-making and working memory (Harvey et al., 2012; Wang, 2008; Wong & Wang, 2006). When the stimulus–response mapping is known during stimulus presentation, we assumed a continuous flow of the evidence accumulation variable to the motor structures that prepare the response, similar to GCD, followed by sustained activity at the motor preparation level during the delay corresponding to the level of cumulative evidence. Gating inhibition at the motor preparation level is increased to prevent muscle activation. RS detection and muscle activation are then achieved by accumulating evidence from the RS, similar to models of one-choice RT tasks (Ratcliff & Van Dongen, 2011; Smith, 1995). When the stimulus–response mapping is not known during stimulus presentation and is instead delivered by the RS,

we assumed that subjects first compute a decision about the category of the stimulus and store this categorical representation in working memory. Motor preparation for a specific response begins after the presentation of the RS, through additional processing operations to convert the categorical representation of the stimulus into a response.

We tested predictions from GCD_{RS} in three experiments that used a RS variant of the random dot motion task featuring a manipulation of motion coherence and a delay between stimulus offset and RS onset. The stimulus–response mapping was known during stimulus presentation in Experiments 1 and 2, and was delivered by the RS in Experiment 3. Experiments 1 and 3 manipulated the duration of the delay (3 s vs. 5 s vs. 7 s), and incorporated FR blocks of trials as a control condition. Experiment 2 manipulated stimulus presentation duration. Empirical findings from FR blocks replicate previous findings, and provide additional evidence for GCD. Specifically, mean PMT and mean MT increased as motion coherence decreased, the latter being caused by a decrease in the slope of muscle activation. Moreover, the rate of partial muscle activation in the EMG channel associated with the response increased as coherence decreased, due to the decrease in the signal-to-noise ratio of the motor preparation variable. Empirical findings from RS blocks were globally in line with predictions from GCD_{RS}. In Experiments 1 and 2, the rate of partial muscle activation during the delay was higher in the EMG channel associated with the response than in the opposite channel, suggesting that subjects maintained a representation of the selected response at the motor preparation level. Consequently, mean PMT was much faster compared to that observed in the FR variant of the task. In Experiment 3, the rate of partial muscle activation during the delay did not differ between the two EMG channels, confirming that subjects did not prepare a specific response before the RS. After the RS, the rate of partial muscle activation was higher in the EMG channel associated with the response than in the opposite channel, reflecting the formation of the motor command. Mean PMT was much slower compared to the previous experiments, due to additional processing operations to convert the categorical representation of the stimulus into a response, according to the mapping provided by the RS.

Experimental manipulations in RS blocks provided further constraints on GCD_{RS}. A decrease in motion coherence produced a decrease in the slope of muscle activation in the three experiments, though the amplitude of this modulation was too small in the first two experiments to impact mean MT. This unexpected finding suggests that subjects accumulated a few samples of motion evidence retrieved from memory. The rate of evidence accumulation in phase 2 (parameter w) thus seems to be determined by two sources of evidence: evidence sampled from the RS and (to a much lesser extent) evidence from the stimulus retrieved from memory. One may be tempted to relate this finding to the recent study of Shushruth et al. (2022), showing that monkeys store samples of evidence in memory and do not accumulate evidence before the presentation of the RS. There are, however, important differences between the two studies. Most importantly, the processing scheme hypothesized by Shushruth et al. (2022) predicts no difference in mean PMT and mean MT between FR and RS blocks. However, findings from Experiments 1 and 3 show a clear difference between the two task variants. Although the amplitude of the difference was reduced in Experiment 3, mean PMT was not modulated by motion coherence, contrary to FR blocks. These findings suggest that (a) motion evidence retrieved from memory cannot be the only source of evidence determining parameter w, and (b) the retrieval process occurs in late processing steps, after the evidence accumulation variable in Phase 2 has crossed the gate. We thus interpret the motion coherence effect on the slope of muscle activation as a final attempt to verify the decision, though follow-up studies are needed to gain a better understanding of this phenomenon.

Although mean PMT was not modulated by motion coherence in Experiment 3, it systematically increased as motion coherence decreased in Experiments 1 and 2. This effect thus appeared to be driven by a modulation of the average level of sustained motor preparation activity by coherence during the delay, consistent with single-unit studies in monkeys (de Lafuente et al., 2015; Kiani et al., 2008; Rao et al., 2012; Roitman & Shadlen, 2002; Shadlen & Newsome, 2001). Specifically, the average level of sustained motor preparation activity decreased as motion coherence decreased. This phenomenon could have been caused by at least three mechanisms (see the general introduction): a short post-threshold evidence accumulation period caused by a delay introduced by the (unknown) neural mechanism that compares activity to the threshold (Mazurek et al., 2003), a threshold that decreases as processing time increases due to the attentional cost of acquiring new samples of evidence (Cisek et al., 2009; Ditterich, 2006a, 2006b; Drugowitsch et al., 2012; Thura et al., 2012), or a mixture of terminated and nonterminated decision processes (Ratcliff, 2006).[11] The manipulation of stimulus presentation duration in Experiment 2 also produced a modulation of mean PMT. Specifically, mean PMT increased as stimulus duration decreased. We do not see how a decreasing threshold with increasing processing time or a short post-threshold evidence accumulation period could explain this effect. The most plausible explanation among the three hypotheses proposed above seems to be the mixture of terminated and nonterminated processes: shorter stimulus presentations increased the proportion of evidence accumulation trajectories that failed to reach the threshold before transitioning to sustained activity, due to a reduced amount of evidence in the processing pipeline. This hypothesis points to a more general problem, which has not yet been resolved in the literature. It is unclear whether the decision-maker has access to partial cumulative evidence or not (Meyer et al., 1985, 1988; Ratcliff, 1988, 2006; Usher & McClelland, 2001). Within GCD_{RS}, this problem could be formulated as follows. If the decision-maker has access to partial cumulative evidence, then the level of cumulated evidence could be maintained at the motor preparation level during the delay. The starting point for the second phase of accumulation would then correspond to this level. If not, then the decision-maker would produce a guess. Motor preparation activity would drop to 0 (baseline level) during the delay, and the starting point for the second phase of accumulation would thus be located farther away from the gate. Although a rigorous test of these two alternative hypotheses requires formal modeling, two aspects of the data from Experiment 2 appear to favor the partial cumulative evidence

[11] One may argue that the probability of nonterminated evidence accumulation trajectories is null for long stimulus presentation durations (such as the 2 s condition in Experiments 1 and 2), making the mixture hypothesis unlikely. To shed light on this issue, we computed the proportion of trials beyond 2 s for each motion coherence condition from FR blocks in Experiment 1. This proportion increased as motion coherence decreased (40% coherence, $M = 2.23\%$; 11% coherence, $M = 10.78\%$; 2% coherence, $M = 18.65\%$). This analysis suggests the mixture hypothesis is plausible, at least in Experiment 1.

hypothesis. First, response accuracy did not differ in the 40% coherence condition between the three stimulus presentation durations (post hoc pairwise comparisons corrected with Holm's procedure: all $ps > .05$). This result is difficult to reconcile with the guessing hypothesis, so long as one assumes that the probability of nonterminated processes is not null in the 40% coherence/0.3 s stimulus presentation condition. The partial cumulative evidence hypothesis appears more plausible, as the level of cumulative evidence for nonterminated processes should be close to the threshold on average. Second, the guessing hypothesis predicts a drop in response accuracy at slow PMTs, because the starting point of motor preparation for guesses should be located farther away from the gate compared to regular trials. The amplitude of this drop should increase as stimulus duration decreases, because the proportion of guesses should increase. One way to evaluate this hypothesis consists in computing the proportion of correct responses as a function of PMT bins. These so-called conditional accuracy functions (Gratton et al., 1988; Luce, 1986) are shown in Appendix D. Conditional accuracy dynamics are very similar across the three stimulus duration conditions, and do not show a clear drop of accuracy for slow PMTs.

Last, the delay manipulation in Experiments 1 and 3 provides insight into temporal preparation mechanisms in RS tasks. As expected, longer delays reduced the quantity/quality of attentional resources allocated to the RS, and the impact of this modulation on performance was detectable only when RS processing was demanding. Specifically, we observed a reliable increase in mean PMT and mean MT as the delay increased in Experiment 3 only, as well as a decrease in the slope of muscle activation, similar to previous findings obtained using the foreperiod paradigm (Hasbroucq et al., 1995; Tandonnet et al., 2003). GCD_{RS} offers a simple explanation for this phenomenon: the decrease in attentional resources allocated to the RS as the delay increases results in a decrease in the quality of evidence accumulated in Phase 2. The lower rate of evidence accumulation w produces an increase in mean PMT and mean MT, and a decrease in the slope of muscle activation. Therefore, GCD_{RS} appears to be a promising tool for further investigation of the processing mechanisms underlying temporal preparation.

Limitations and Future Directions

To our knowledge, this work constitutes the first attempt to extend continuous flow models proposed in the context of immediate decision reports to delayed decision reports in humans. It is also the first EMG investigation of muscle activity in RS tasks. Three limitations restrict its scope, but we see these limitations as directions for future research rather than theoretical or methodological flaws.

A first limitation concerns the absence of continuous neurophysiological signals at the motor preparation level to test latent assumptions of GCD_{RS}, and one may question the extent to which the model is falsifiable without such signals. Note, however, that we have allowed room for model falsification at several occasions. For instance, having failed to observe a difference in the rate of partial muscle activation between the two EMG channels during the delay in Experiments 1 and 2 would have provided evidence against a maintenance of the choice at the motor preparation level. Having observed similar mean PMT and mean MT in RS and FR blocks in Experiments 1 and 3 would have provided evidence against an accumulation of evidence before the RS, and would have favored the alternative processing scheme observed in monkeys by Shushruth et al. (2022). Still, one may wonder if a prolongation of evidence accumulation until the onset of the RS would predict similar effects to GCD_{RS} at the behavioral and EMG levels. Apart from the fact that this hypothetical mechanism has never been observed by previous neurophysiological studies in both monkeys and humans (see the general introduction) and would lead to neural firing rates so high that they would likely exceed biological limits, it can be refuted on the basis of two arguments. First, we acknowledge that some samples of motion evidence may remain in the processing pipeline when the stimulus disappears due to sensory delays, and these samples may be accumulated during the memory delay (Resulaj et al., 2009). However, sensory delays in the random dot motion task are much shorter (<0.3 s; Kiani et al., 2008; Resulaj et al., 2009; Roitman & Shadlen, 2002) than memory delays used in the present work (3–7 s), so the stream of evidence from the stimulus appears insufficient to support an accumulation on such long timescales. Second, assuming that participants could *somehow* continue to accumulate motion evidence during the 3–7 s memory delay, perhaps through repeated sampling from memory, the level of cumulative evidence—and hence response accuracy—should increase with increasing delays. However, the data from Experiments 1 and 3 provide substantial to strong evidence against an effect of delay on response accuracy and strong to decisive evidence against an interaction between delay and coherence.

Although continuous neurophysiological signals at the motor preparation level do not appear to be critical for falsifying the basic processing assumptions of GCD_{RS}, they will provide a stronger test of the model and may lead to theoretical developments. EEG, in particular, offers two markers of motor preparation in the case of left/right manual responses: the lateralized readiness potential and the decrease in spectral activity in the μ/β band over the motor cortex (de Jong et al., 1988; Gratton et al., 1988; Pfurtscheller & Lopes da Silva, 1999). While both signals have been interpreted as reflecting evidence accumulation (e.g., Gluth et al., 2013; Kelly et al., 2021; Kelly & O'Connell, 2013; Lui et al., 2021; O'Connell et al., 2012; Servant et al., 2016; Steinemann et al., 2018), recent studies suggest that the lateralized readiness potential is silent in RS tasks during the presentation of the stimulus and the memory delay, while the μ/β signals exhibit ramping dynamics followed by sustained asymptotic activity (Rogge et al., 2022; Twomey et al., 2016). Therefore, the latter seems a good candidate to further test motor preparation dynamics assumed by GCD_{RS} in humans. The EEG technique, however, is not well suited to the analysis of tasks featuring very long trials, due to the high probability of movement and electrical artifacts, though blind source separation methods could be applied to mitigate this issue (e.g., Onton et al., 2006). Moreover, the poor signal-to-noise ratio of EEG makes trial-by-trial signal analysis difficult (but not impossible; e.g., Nunez et al., 2017; Ratcliff, Sederberg, et al., 2016). Therefore, we believe that EEG investigations of delayed decision reports should be conducted in tandem with EMG.

A second limitation concerns the absence of mathematical modeling of the data. An important strength of current continuous flow evidence accumulation models is their mathematical formalization, which makes mechanistic assumptions explicit and predictions clear (Lewandowsky & Farrell, 2011). This formalization, however, requires solving detailed and complex mechanistic problems, such as the transition between evidence accumulation and

sustained activity within GCD_{RS}, taking into account the mechanics of the Kalman-Bucy filter at the motor preparation level. Since the goal of the present work was to extend general processing aspects of immediate decision reports to delayed decision reports, this step appeared premature, but we believe that it is necessary for future model developments and applications. An important challenge concerns the small amount of available data given the complexity of the model. In essence, the RS paradigm used in the present work offers no behavioral data prior to the RS to constrain model parameters. Consequently, we doubt that model parameters will be identifiable if GCD_{RS} is fit to behavioral data only. We see two complementary ways to mitigate this problem. First, the original GCD could be fit to data from FR blocks, and the rate of evidence accumulation during stimulus presentation could be used to reduce the degrees of freedom within GCD_{RS}. Second, electrophysiological data could help constrain the model. For instance, the rate of partial muscle activation could be incorporated into the loss function quantifying the discrepancy between data and model predictions (Dendauw et al., 2024). However, partial muscle activations will provide little constraints on the model when the stimulus–response mapping is delivered by the RS, so we believe that the best strategy would be to constrain GCD_{RS} with both EMG and EEG data.

Finally, the scope of GCD_{RS} is currently limited to short delays between decisions and actions. An important task for future research will be to extend the model's scope to longer delays, involving long-term memory. Since the choice cannot be actively maintained in the form of sustained activity over long periods of time, it must be stored using different neurophysiological mechanisms (e.g., long-term potentiation and depression; Abraham et al., 2019). The present work suggests that subjects store samples of evidence as well, presumably to be able to check the initial choice. This strategy appears particularly important in the context of long delays, because it will allow subjects to recompute—and potentially revise—the choice, taking into account new events that have occurred during the delay.

Constraints on Generality

Participants in the three experiments were healthy students from the University of Franche-Comté (mostly psychology undergraduates), whereas the target population was much larger (healthy young adults). Thus, convenience sampling was used, mainly due to the constraints of conducting electrophysiological recordings. Importantly, we see no theoretical reason why this sampling bias could lead to a misleading picture of the neurocognitive mechanisms underlying delayed decision reports investigated in the present work. Another bias to consider is the selection of right-handed participants. Left- and right-handed subjects are likely to have a different mean motor time for left and right manual responses, so the choice of right-handed subjects was made to avoid an additional factor to consider in the statistical analyses, and additional complexities inherent to mixed designs. We see no theoretical reason why this handedness effect could interact with the factors manipulated in the present experiments, but this might be something worth investigating in future studies. Finally, delayed decision reports were studied in the context of a RS variant of the random dot motion task for the reasons explained in the general introduction section. Because random dot stimuli vary in time and space, one may wonder whether the present findings replicate with static stimuli that are very common in the experimental psychology literature. In this respect, we note that predictions from GCD_{RS} would remain similar.

References

Abraham, W. C., Jones, O. D., & Glanzman, D. L. (2019). Is plasticity of synapses the mechanism of long-term memory storage? *NPJ Science of Learning*, *4*(1), Article 9. https://doi.org/10.1038/s41539-019-0048-y

Balsdon, T., Verdonck, S., Loossens, T., & Philiastides, M. G. (2023). Secondary motor integration as a final arbiter in sensorimotor decision-making. *PLOS Biology*, *21*(7), Article e3002200. https://doi.org/10.1371/journal.pbio.3002200

Bennur, S., & Gold, J. I. (2011). Distinct representations of a perceptual decision and the associated oculomotor plan in the monkey lateral intraparietal area. *The Journal of Neuroscience*, *31*(3), 913–921. https://doi.org/10.1523/JNEUROSCI.4417-10.2011

Buc Calderon, C., Verguts, T., & Gevers, W. (2015). Losing the boundary: Cognition biases action well after action selection. *Journal of Experimental Psychology: General*, *144*(4), 737–743. https://doi.org/10.1037/xge0000087

Burle, B., Tandonnet, C., & Hasbroucq, T. (2010). Excitatory and inhibitory motor mechanisms of temporal preparation. In A. C. Nobre & J. T. Coull (Eds.), *Attention and time* (pp. 243–256). Oxford University Press. https://doi.org/10.1093/acprof:oso/9780199563456.003.0018

Calderon, C. B., Gevers, W., & Verguts, T. (2018). The unfolding action model of initiation times, movement times, and movement paths. *Psychological Review*, *125*(5), 785–805. https://doi.org/10.1037/rev0000110

Campbell, J. I. D., & Thompson, V. A. (2012). MorePower 6.0 for ANOVA with relational confidence intervals and Bayesian analysis. *Behavior Research Methods*, *44*(4), 1255–1265. https://doi.org/10.3758/s13428-012-0186-0

Chapman, C. S., Gallivan, J. P., Wood, D. K., Milne, J. L., Culham, J. C., & Goodale, M. A. (2010). Reaching for the unknown: Multiple target encoding and real-time decision-making in a rapid reach task. *Cognition*, *116*(2), 168–176. https://doi.org/10.1016/j.cognition.2010.04.008

Cisek, P., Puskas, G. A., & El-Murr, S. (2009). Decisions in changing conditions: The urgency-gating model. *The Journal of Neuroscience*, *29*(37), 11560–11571. https://doi.org/10.1523/JNEUROSCI.1844-09.2009

Coallier, É., & Kalaska, J. F. (2014). Reach target selection in humans using ambiguous decision cues containing variable amounts of conflicting sensory evidence supporting each target choice. *Journal of Neurophysiology*, *112*(11), 2916–2938. https://doi.org/10.1152/jn.00145.2014

Coles, M. G. (1989). Modern mind-brain reading: Psychophysiology, physiology, and cognition. *Psychophysiology*, *26*(3), 251–269. https://doi.org/10.1111/j.1469-8986.1989.tb01916.x

Correa, A., Lupiáñez, J., Madrid, E., & Tudela, P. (2006). Temporal attention enhances early visual processing: A review and new evidence from event-related potentials. *Brain Research*, *1076*(1), 116–128. https://doi.org/10.1016/j.brainres.2005.11.074

de Jong, R., Wierda, M., Mulder, G., & Mulder, L. J. (1988). Use of partial stimulus information in response processing. *Journal of Experimental Psychology: Human Perception and Performance*, *14*(4), 682–692. https://doi.org/10.1037/0096-1523.14.4.682

de Lafuente, V., Jazayeri, M., & Shadlen, M. N. (2015). Representation of accumulating evidence for a decision in two parietal areas. *The Journal of Neuroscience*, *35*(10), 4306–4318. https://doi.org/10.1523/JNEUROSCI.2451-14.2015

de Lange, F. P., Rahnev, D. A., Donner, T. H., & Lau, H. (2013). Prestimulus oscillatory activity over motor cortex reflects perceptual expectations. *The Journal of Neuroscience*, *33*(4), 1400–1410. https://doi.org/10.1523/JNEUROSCI.1094-12.2013

Dendauw, E., Evans, N. J., Logan, G. D., Haffen, E., Bennabi, D., Gajdos, T., & Servant, M. (2024). The gated cascade diffusion model: An integrated theory of decision making, motor preparation, and motor execution. *Psychological Review*, *131*(4), 825–857. https://doi.org/10.1037/rev0000464

Ditterich, J. (2006a). Evidence for time-variant decision making. *European Journal of Neuroscience*, *24*(12), 3628–3641. https://doi.org/10.1111/j.1460-9568.2006.05221.x

Ditterich, J. (2006b). Stochastic models of decisions about motion direction: Behavior and physiology. *Neural Networks*, *19*(8), 981–1012. https://doi.org/10.1016/j.neunet.2006.05.042

Donner, T. H., Siegel, M., Fries, P., & Engel, A. K. (2009). Buildup of choice-predictive activity in human motor cortex during perceptual decision making. *Current Biology*, *19*(18), 1581–1585. https://doi.org/10.1016/j.cub.2009.07.066

Drugowitsch, J., Moreno-Bote, R., Churchland, A. K., Shadlen, M. N., & Pouget, A. (2012). The cost of accumulating evidence in perceptual decision making. *The Journal of Neuroscience*, *32*(11), 3612–3628. https://doi.org/10.1523/JNEUROSCI.4010-11.2012

Eriksen, C. W., Coles, M. G. H., Morris, L. R., & O'hara, W. P. (1985). An electromyographic examination of response competition. *Bulletin of the Psychonomic Society*, *23*(3), 165–168. https://doi.org/10.3758/BF03329816

Eriksen, C. W., & Eriksen, B. A. (1979). Target redundancy in visual search: Do repetitions of the target within thedisplay impair processing? *Perception & Psychophysics*, *26*(3), 195–205. https://doi.org/10.3758/BF03199869

Forstmann, B. U., Ratcliff, R., & Wagenmakers, E.-J. (2016). Sequential sampling models in cognitive neuroscience: Advantages, applications, and extensions. *Annual Review of Psychology*, *67*(1), 641–666. https://doi.org/10.1146/annurev-psych-122414-033645

Friedman, J., Brown, S., & Finkbeiner, M. (2013). Linking cognitive and reaching trajectories via intermittent movement control. *Journal of Mathematical Psychology*, *57*(3–4), 140–151. https://doi.org/10.1016/j.jmp.2013.06.005

Gluth, S., Rieskamp, J., & Büchel, C. (2013). Classic EEG motor potentials track the emergence of value-based decisions. *NeuroImage*, *79*, 394–403. https://doi.org/10.1016/j.neuroimage.2013.05.005

Gold, J. I., & Shadlen, M. N. (2000). Representation of a perceptual decision in developing oculomotor commands. *Nature*, *404*(6776), 390–394. https://doi.org/10.1038/35006062

Gold, J. I., & Shadlen, M. N. (2003). The influence of behavioral context on the representation of a perceptual decision in developing oculomotor commands. *The Journal of Neuroscience*, *23*(2), 632–651. https://doi.org/10.1523/JNEUROSCI.23-02-00632.2003

Gold, J. I., & Shadlen, M. N. (2007). The neural basis of decision making. *Annual Review of Neuroscience*, *30*(1), 535–574. https://doi.org/10.1146/annurev.neuro.29.051605.113038

Gratton, G., Coles, M. G., Sirevaag, E. J., Eriksen, C. W., & Donchin, E. (1988). Pre- and poststimulus activation of response channels: A psychophysiological analysis. *Journal of Experimental Psychology: Human Perception and Performance*, *14*(3), 331–344. https://doi.org/10.1037/0096-1523.14.3.331

Hanes, D. P., & Schall, J. D. (1996). Neural control of voluntary movement initiation. *Science*, *274*(5286), 427–430. https://doi.org/10.1126/science.274.5286.427

Hanks, T. D., & Summerfield, C. (2017). Perceptual decision making in rodents, monkeys, and humans. *Neuron*, *93*(1), 15–31. https://doi.org/10.1016/j.neuron.2016.12.003

Harvey, C. D., Coen, P., & Tank, D. W. (2012). Choice-specific sequences in parietal cortex during a virtual-navigation decision task. *Nature*, *484*(7392), 62–68. https://doi.org/10.1038/nature10918

Hasbroucq, T., Mouret, I., Seal, J., & Akamatsu, M. (1995). Finger pairings in two-choice reaction time tasks: Does the between-hands advantage reflect response preparation? *Journal of Motor Behavior*, *27*(3), 251–262. https://doi.org/10.1080/00222895.1995.9941715

Heitz, R. P., & Schall, J. D. (2012). Neural mechanisms of speed–accuracy tradeoff. *Neuron*, *76*(3), 616–628. https://doi.org/10.1016/j.neuron.2012.08.030

Horwitz, G. D., & Newsome, W. T. (1999). Separate signals for target selection and movement specification in the superior colliculus. *Science*, *284*(5417), 1158–1161. https://doi.org/10.1126/science.284.5417.1158

Kelly, S. P., Corbett, E. A., & O'Connell, R. G. (2021). Neurocomputational mechanisms of prior-informed perceptual decision-making in humans. *Nature Human Behaviour*, *5*(4), 467–481. https://doi.org/10.1038/s41562-020-00967-9

Kelly, S. P., & O'Connell, R. G. (2013). Internal and external influences on the rate of sensory evidence accumulation in the human brain. *The Journal of Neuroscience*, *33*(50), 19434–19441. https://doi.org/10.1523/JNEUROSCI.3355-13.2013

Kelly, S. P., & O'Connell, R. G. (2015). The neural processes underlying perceptual decision making in humans: Recent progress and future directions. *Journal of Physiology, Paris*, *109*(1–3), 27–37. https://doi.org/10.1016/j.jphysparis.2014.08.003

Kiani, R., Hanks, T. D., & Shadlen, M. N. (2008). Bounded integration in parietal cortex underlies decisions even when viewing duration is dictated by the environment. *The Journal of Neuroscience*, *28*(12), 3017–3029. https://doi.org/10.1523/JNEUROSCI.4761-07.2008

Kinder, K. T., Buss, A. T., & Tas, A. C. (2022). Tracking flanker task dynamics: Evidence for continuous attentional selectivity. *Journal of Experimental Psychology: Human Perception and Performance*, *48*(7), 771–781. https://doi.org/10.1037/xhp0001023

LaBerge, D. (1962). A recruitment theory of simple behavior. *Psychometrika*, *27*(4), 375–396. https://doi.org/10.1007/BF02289645

Laming, D. R. J. (1968). *Information theory of choice-reaction times*. Academic Press.

Lepora, N. F., & Pezzulo, G. (2015). Embodied choice: How action influences perceptual decision making. *PLOS Computational Biology*, *11*(4), Article e1004110. https://doi.org/10.1371/journal.pcbi.1004110

Lewandowsky, S., & Farrell, S. (2011). *Computational modeling in cognition: Principles and practice*. Sage Publications. https://doi.org/10.4135/9781483349428

Liu, J., & Liu, Q. (2016). Use of the integrated profile for voluntary muscle activity detection using EMG signals with spurious background spikes: A study with incomplete spinal cord injury. *Biomedical Signal Processing and Control*, *24*, 19–24. https://doi.org/10.1016/j.bspc.2015.09.004

Luce, R. D. (1986). *Response times: Their role in inferring elementary mental organization*. Oxford University Press.

Lui, K. K., Nunez, M. D., Cassidy, J. M., Vandekerckhove, J., Cramer, S. C., & Srinivasan, R. (2021). Timing of readiness potentials reflect a decision-making process in the human brain. *Computational Brain & Behavior*, *4*(3), 264–283. https://doi.org/10.1007/s42113-020-00097-5

Masse, N. Y., Rosen, M. C., & Freedman, D. J. (2020). Reevaluating the role of persistent neural activity in short-term memory. *Trends in Cognitive Sciences*, *24*(3), 242–258. https://doi.org/10.1016/j.tics.2019.12.014

Mazurek, M. E., Roitman, J. D., Ditterich, J., & Shadlen, M. N. (2003). A role for neural integrators in perceptual decision making. *Cerebral Cortex*, *13*(11), 1257–1269. https://doi.org/10.1093/cercor/bhg097

McClelland, J. L. (1979). On the time relations of mental processes: An examination of systems of processes in cascade. *Psychological Review*, *86*(4), 287–330. https://doi.org/10.1037/0033-295X.86.4.287

Meyer, D. E., Irwin, D. E., Osman, A. M., & Kounois, J. (1988). The dynamics of cognition and action: Mental processes inferred from speed–accuracy decomposition. *Psychological Review*, *95*(2), 183–237. https://doi.org/10.1037/0033-295X.95.2.183

Meyer, D. E., Yantis, S., Osman, A. M., & Smith, J. E. (1985). Temporal properties of human information processing: Tests of discrete versus continuous models. *Cognitive Psychology*, *17*(4), 445–518. https://doi.org/10.1016/0010-0285(85)90016-7

Nakayama, K., Moher, J., & Song, J.-H. (2023). Rethinking vision and action. *Annual Review of Psychology*, *74*(1), 59–86. https://doi.org/10.1146/annurev-psych-021422-043229

Nunez, M. D., Vandekerckhove, J., & Srinivasan, R. (2017). How attention influences perceptual decision making: Single-trial EEG correlates of drift-diffusion model parameters. *Journal of Mathematical Psychology*, *76*(Part B), 117–130. https://doi.org/10.1016/j.jmp.2016.03.003

O'Connell, R. G., Dockree, P. M., & Kelly, S. P. (2012). A supramodal accumulation-to-bound signal that determines perceptual decisions in humans. *Nature Neuroscience*, *15*(12), 1729–1735. https://doi.org/10.1038/nn.3248

O'Connell, R. G., & Kelly, S. P. (2021). Neurophysiology of human perceptual decision-making. *Annual Review of Neuroscience*, *44*(1), 495–516. https://doi.org/10.1146/annurev-neuro-092019-100200

Onton, J., Westerfield, M., Townsend, J., & Makeig, S. (2006). Imaging human EEG dynamics using independent component analysis. *Neuroscience and Biobehavioral Reviews*, *30*(6), 808–822. https://doi.org/10.1016/j.neubiorev.2006.06.007

Peirce, J., Gray, J. R., Simpson, S., MacAskill, M., Höchenberger, R., Sogo, H., Kastman, E., & Lindeløv, J. K. (2019). PsychoPy2: Experiments in behavior made easy. *Behavior Research Methods*, *51*(1), 195–203. https://doi.org/10.3758/s13428-018-01193-y

Pfurtscheller, G., & Lopes da Silva, F. H. (1999). Event-related EEG/MEG synchronization and desynchronization: Basic principles. *Clinical Neurophysiology*, *110*(11), 1842–1857. https://doi.org/10.1016/S1388-2457(99)00141-8

Purcell, B. A., Heitz, R. P., Cohen, J. Y., Schall, J. D., Logan, G. D., & Palmeri, T. J. (2010). Neurally constrained modeling of perceptual decision making. *Psychological Review*, *117*(4), 1113–1143. https://doi.org/10.1037/a0020311

Purcell, B. A., Schall, J. D., Logan, G. D., & Palmeri, T. J. (2012). From salience to saccades: Multiple-alternative gated stochastic accumulator model of visual search. *The Journal of Neuroscience*, *32*(10), 3433–3446. https://doi.org/10.1523/JNEUROSCI.4622-11.2012

Rao, V., DeAngelis, G. C., & Snyder, L. H. (2012). Neural correlates of prior expectations of motion in the lateral intraparietal and middle temporal areas. *The Journal of Neuroscience*, *32*(29), 10063–10074. https://doi.org/10.1523/JNEUROSCI.5948-11.2012

Ratcliff, R. (1988). Continuous versus discrete information processing modeling accumulation of partial information. *Psychological Review*, *95*(2), 238–255. https://doi.org/10.1037/0033-295X.95.2.238

Ratcliff, R. (2006). Modeling response signal and response time data. *Cognitive Psychology*, *53*(3), 195–237. https://doi.org/10.1016/j.cogpsych.2005.10.002

Ratcliff, R., Sederberg, P., Smith, T., & Childers, R. (2016). A single trial analysis of EEG in recognition memory: Tracking the neural correlates of memory strength. *Neuropsychologia*, *93*(Part A), 128–141. https://doi.org/10.1016/j.neuropsychologia.2016.09.026

Ratcliff, R., & Smith, P. L. (2004). A comparison of sequential sampling models for two-choice reaction time. *Psychological Review*, *111*(2), 333–367. https://doi.org/10.1037/0033-295X.111.2.333

Ratcliff, R., Smith, P. L., Brown, S. D., & McKoon, G. (2016). Diffusion decision model: Current issues and history. *Trends in Cognitive Sciences*, *20*(4), 260–281. https://doi.org/10.1016/j.tics.2016.01.007

Ratcliff, R., & Van Dongen, H. P. A. (2011). Diffusion model for one-choice reaction-time tasks and the cognitive effects of sleep deprivation. *Proceedings of the National Academy of Sciences of the United States of America*, *108*(27), 11285–11290. https://doi.org/10.1073/pnas.1100483108

Reppert, T. R., Servant, M., Heitz, R. P., & Schall, J. D. (2018). Neural mechanisms of speed–accuracy tradeoff of visual search: Saccade vigor, the origin of targeting errors, and comparison of the superior colliculus and frontal eye field. *Journal of Neurophysiology*, *120*(1), 372–384. https://doi.org/10.1152/jn.00887.2017

Requin, J., Brener, J., & Ring, C. (1991). Preparation for action. In J. R. Jennings & M. G. H. Coles (Eds.), *Handbook of cognitive psychophysiology: Central and autonomic nervous system approaches* (pp. 357–448). Wiley.

Resulaj, A., Kiani, R., Wolpert, D. M., & Shadlen, M. N. (2009). Changes of mind in decision-making. *Nature*, *461*(7261), 263–266. https://doi.org/10.1038/nature08275

Rogge, J., Jocham, G., & Ullsperger, M. (2022). Motor cortical signals reflecting decision making and action preparation. *NeuroImage*, *263*, Article 119667. https://doi.org/10.1016/j.neuroimage.2022.119667

Roitman, J. D., & Shadlen, M. N. (2002). Response of neurons in the lateral intraparietal area during a combined visual discrimination reaction time task. *The Journal of Neuroscience*, *22*(21), 9475–9489. https://doi.org/10.1523/JNEUROSCI.22-21-09475.2002

Rolke, B. (2008). Temporal preparation facilitates perceptual identification of letters. *Perception & Psychophysics*, *70*(7), 1305–1313. https://doi.org/10.3758/PP.70.7.1305

Rolke, B., & Ulrich, R. (2010). On the locus of temporal preparation: Enhancement of premotor processes? In A. C. Nobre & J. T. Coull (Eds.), *Attention and time* (pp. 227–242). Oxford University Press. https://doi.org/10.1093/acprof:oso/9780199563456.003.0017

Santello, M., & McDonagh, M. J. (1998). The control of timing and amplitude of EMG activity in landing movements in humans. *Experimental Physiology*, *83*(6), 857–874. https://doi.org/10.1113/expphysiol.1998.sp004165

Schall, J. D. (2019). Accumulators, neurons, and response time. *Trends in Neurosciences*, *42*(12), 848–860. https://doi.org/10.1016/j.tins.2019.10.001

Seibold, V. C., Balke, J., & Rolke, B. (2023). Temporal attention. *Frontiers in Cognition*, *2*, Article 1168320. https://doi.org/10.3389/fcogn.2023.1168320

Servant, M., Logan, G. D., Gajdos, T., & Evans, N. J. (2021). An integrated theory of deciding and acting. *Journal of Experimental Psychology: General*, *150*(12), 2435–2454. https://doi.org/10.1037/xge0001063

Servant, M., Tillman, G., Schall, J. D., Logan, G. D., & Palmeri, T. J. (2019). Neurally constrained modeling of speed–accuracy tradeoff during visual search: Gated accumulation of modulated evidence. *Journal of Neurophysiology*, *121*(4), 1300–1314. https://doi.org/10.1152/jn.00507.2018

Servant, M., White, C., Montagnini, A., & Burle, B. (2015). Using covert response activation to test latent assumptions of formal decision-making models in humans. *The Journal of Neuroscience*, *35*(28), 10371–10385. https://doi.org/10.1523/JNEUROSCI.0078-15.2015

Servant, M., White, C., Montagnini, A., & Burle, B. (2016). Linking theoretical decision-making mechanisms in the Simon task with electrophysiological data: A model-based neuroscience study in humans. *Journal of Cognitive Neuroscience*, *28*(10), 1501–1521. https://doi.org/10.1162/jocn_a_00989

Shadlen, M. N., & Newsome, W. T. (2001). Neural basis of a perceptual decision in the parietal cortex (area LIP) of the rhesus monkey. *Journal of Neurophysiology*, *86*(4), 1916–1936. https://doi.org/10.1152/jn.2001.86.4.1916

Shushruth, S., Zylberberg, A., & Shadlen, M. N. (2022). Sequential sampling from memory underlies action selection during abstract decision-making. *Current Biology*, *32*(9), 1949–1960.e5. https://doi.org/10.1016/j.cub.2022.03.014

Smith, P. L. (1995). Psychophysically principled models of visual simple reaction time. *Psychological Review*, *102*(3), 567–593. https://doi.org/10.1037/0033-295X.102.3.567

Song, J.-H., & Nakayama, K. (2009). Hidden cognitive states revealed in choice reaching tasks. *Trends in Cognitive Sciences*, *13*(8), 360–366. https://doi.org/10.1016/j.tics.2009.04.009

Steinemann, N. A., O'Connell, R. G., & Kelly, S. P. (2018). Decisions are expedited through multiple neural adjustments spanning the sensorimotor hierarchy. *Nature Communications*, *9*(1), Article 3627. https://doi.org/10.1038/s41467-018-06117-0

Stone, M. (1960). Models for choice-reaction time. *Psychometrika*, *25*(3), 251–260. https://doi.org/10.1007/BF02289729

Tandonnet, C., Burle, B., Vidal, F., & Hasbroucq, T. (2003). The influence of time preparation on motor processes assessed by surface Laplacian estimation. *Clinical Neurophysiology*, *114*(12), 2376–2384. https://doi.org/10.1016/S1388-2457(03)00253-0

Thura, D. (2020). Decision urgency invigorates movement in humans. *Behavioural Brain Research*, *382*, Article 112477. https://doi.org/10.1016/j.bbr.2020.112477

Thura, D., Beauregard-Racine, J., Fradet, C.-W., & Cisek, P. (2012). Decision making by urgency gating: Theory and experimental support. *Journal of Neurophysiology*, *108*(11), 2912–2930. https://doi.org/10.1152/jn.01071.2011

Thura, D., & Cisek, P. (2014). Deliberation and commitment in the premotor and primary motor cortex during dynamic decision making. *Neuron*, *81*(6), 1401–1416. https://doi.org/10.1016/j.neuron.2014.01.031

Thura, D., & Cisek, P. (2016). Modulation of premotor and primary motor cortical activity during volitional adjustments of speed–accuracy trade-offs. *The Journal of Neuroscience*, *36*(3), 938–956. https://doi.org/10.1523/JNEUROSCI.2230-15.2016

Twomey, D. M., Kelly, S. P., & O'Connell, R. G. (2016). Abstract and effector-selective decision signals exhibit qualitatively distinct dynamics before delayed perceptual reports. *The Journal of Neuroscience*, *36*(28), 7346–7352. https://doi.org/10.1523/JNEUROSCI.4162-15.2016

Twomey, D. M., Murphy, P. R., Kelly, S. P., & O'Connell, R. G. (2015). The classic P300 encodes a build-to-threshold decision variable. *European Journal of Neuroscience*, *42*(1), 1636–1643. https://doi.org/10.1111/ejn.12936

Usher, M., & McClelland, J. L. (2001). The time course of perceptual choice: The leaky, competing accumulator model. *Psychological Review*, *108*(3), 550–592. https://doi.org/10.1037/0033-295X.108.3.550

Verdonck, S., Loossens, T., & Philiastides, M. G. (2021). The Leaky Integrating Threshold and its impact on evidence accumulation models of choice response time (RT). *Psychological Review*, *128*(2), 203–221. https://doi.org/10.1037/rev0000258

Vigotsky, A. D., Halperin, I., Lehman, G. J., Trajano, G. S., & Vieira, T. M. (2018). Interpreting signal amplitudes in surface electromyography studies in sport and rehabilitation sciences. *Frontiers in Physiology*, *8*, Article 985. https://doi.org/10.3389/fphys.2017.00985

Wang, X.-J. (2008). Decision making in recurrent neuronal circuits. *Neuron*, *60*(2), 215–234. https://doi.org/10.1016/j.neuron.2008.09.034

Wong, K.-F., & Wang, X.-J. (2006). A recurrent network mechanism of time integration in perceptual decisions. *The Journal of Neuroscience*, *26*(4), 1314–1328. https://doi.org/10.1523/JNEUROSCI.3733-05.2006

Woodrow, H. (1914). The measurement of attention. *The Psychological Monographs*, *17*(5), i–158. https://doi.org/10.1037/h0093087

(*Appendices follow*)

Appendix A

Illustration of Partial Muscle Activations During the Premotor Time in FR Trials (Left Column) and During the Delay in RS Trials (Right Column)

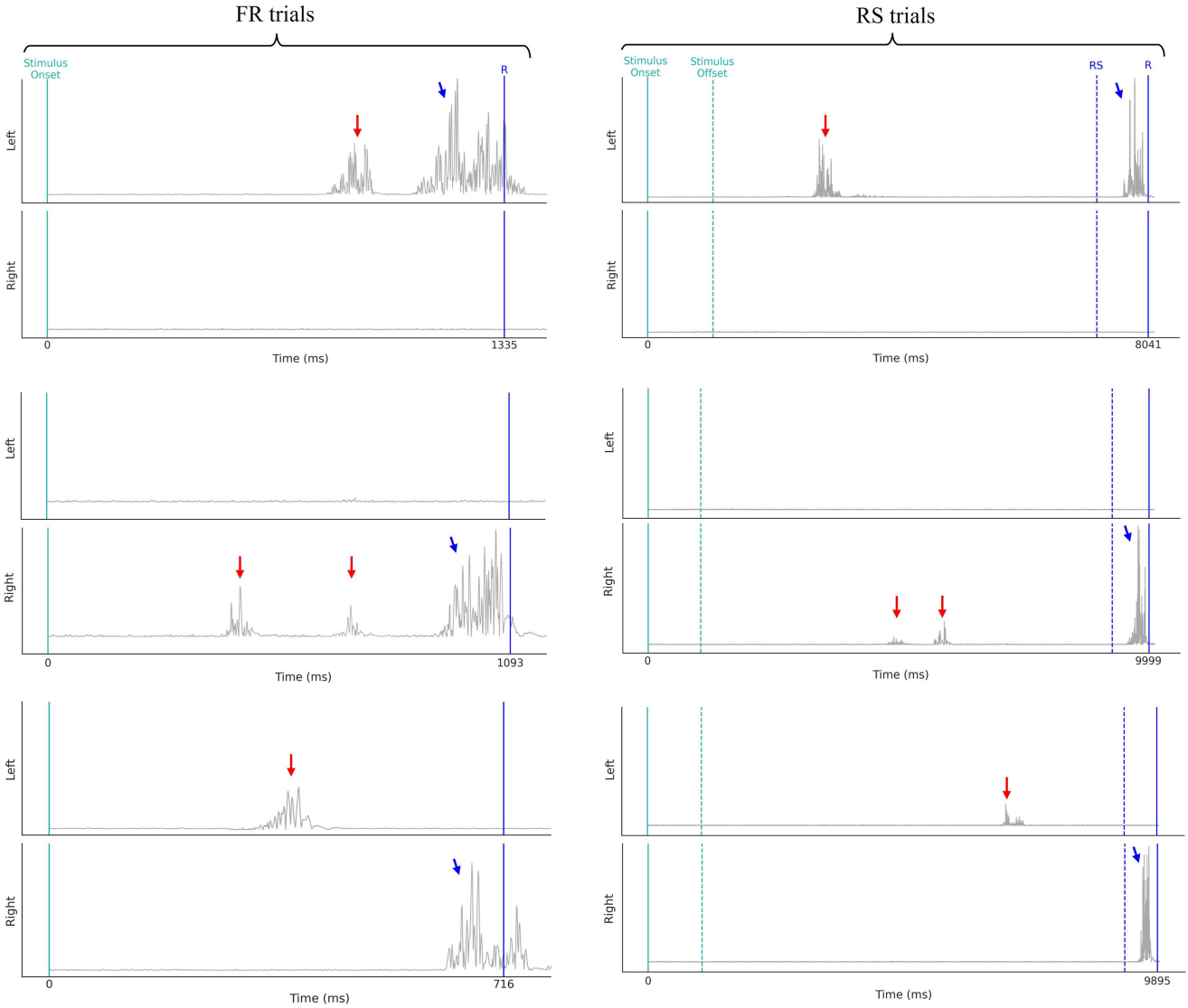

Note. Each of the six subplots represents a trial containing at least one partial muscle activation. The upper EMG signal corresponds to the left hand, and the lower EMG signal corresponds to the right hand. The green solid vertical line corresponds to the onset of the stimulus. The blue solid vertical line corresponds to the response, and the number below corresponds to the reaction time (the timescale is thus different between subplots). Each partial muscle activation is indicated by a red arrow. The activation of the muscle leading to the response is indicated by a blue arrow. In RS trials, the offset of the stimulus is represented by a green vertical dashed line, and the onset of the RS is represented by a blue vertical dashed line. FR = free response; RS = response signal; EMG = electromyography. See the online article for the color version of this figure.

(*Appendices continue*)

Appendix B

EMG Onset Detection

In each experiment, we applied the following three-step method to the rectified EMG signals to detect onsets. The first step allowed us to identify time windows of active EMG activity. For each epoch and EMG channel, we first computed the mean M_b and standard deviation SD_b of the signal in the baseline period (from the beginning of the epoch to stimulus onset). Time windows of EMG activity corresponded to time windows in which the amplitude of the signal exceeded the following criterion:

$$\text{criterion} = M_b + 7 \times SD_b. \quad \text{(B1)}$$

This algorithm was applied to the entire epoch. Due to the oscillatory nature of EMG activity, the amplitude of the signal can sometimes fall below the criterion during an EMG burst. We thus merged consecutive time windows of EMG activity separated by less than 0.025 s. To further increase the robustness of EMG detection in the presence of background noise, we discarded periods of active EMG activity with a duration $<n + 3$ samples (since the sampling frequency of our recordings is 1,024 Hz, one sample corresponds to 0.98 ms), where n corresponded to the number of time windows per second with a duration <7 samples (estimated on the whole epoch). Finally, we removed time windows before stimulus onset and after the response. This algorithm has the advantage of making minimal assumptions regarding the minimal duration of an EMG burst (because there is no theory specifying how long an EMG burst should be) while increasing the detection criterion in the presence of background noise.

The above method allowed us to identify time windows of active EMG activity, but it is known to overestimate EMG onsets (especially when a conservative criterion is used). To address this problem, we applied the EMG onset detection algorithm proposed by Santello and McDonagh (1998) to each window (see also Liu & Liu, 2016). Finally, all triggers relative to stimulus and response identification were removed, and each trial was visually inspected by the experimenter. Erroneous EMG onsets were manually corrected.

Appendix C

Statistical Results Relative to Model Predictions

Table C1
Summary of Statistical Tests of GCD and GCD_{RS} Predictions (Experiment 1)

Dependent variable	Effect tested	p significance	Hypothesis favored by the inclusion Bayes factor and corresponding strength of evidence
Response accuracy (all blocks)	Block Type × Coherence	[a]	H_1, decisive
Response accuracy (RS blocks)	Delay		H_0, substantial
	Delay × Coherence		H_0, strong
Mean MT (all blocks)	Block Type × Coherence	[a]	H_1, decisive
Mean MT (RS blocks)	Coherence		H_0, substantial
	Delay × Coherence		H_0, anecdotal
Slope of muscle activation (all blocks)	Block Type × Coherence	[a]	H_1, decisive
Slope of muscle activation (RS blocks)	Coherence	[a]	H_1, strong
	Delay		H_0, substantial
	Delay × Coherence		H_0, strong
Mean PMT (all blocks)	Block Type × Coherence	[a]	H_1, decisive
Mean PMT (RS blocks)	Coherence	[a]	H_1, substantial
	Delay		H_0, anecdotal
	Delay × Coherence		H_0, anecdotal
Rate of PMA in the EMG channel associated with the response (FR blocks)	Coherence	[a]	H_1, decisive
Rate of PMA during the delay (RS blocks)	EMG channel	[a]	H_1, strong
Rate of PMA in the EMG channel associated with the response during the delay (RS blocks)	Coherence		H_0, anecdotal
	Delay		H_0, anecdotal
	Delay × Coherence		H_0, substantial

Note. Categories used to classify the strength of evidence correspond to those defined in the main text. RS = response signal; FR = free response; MT = motor time; PMT = premotor time; PMA = partial motor activation; EMG = electromyography; GCD = gated cascade diffusion model; GCD_{RS} = GCD extension for response signal tasks.
[a] Significant p value at the $\alpha = .05$ threshold level.

(*Appendices continue*)

Table C2

Summary of Statistical Tests of GCD_{RS} Predictions (Experiment 2)

Dependent variable	Effect tested	*p* significance	Hypothesis favored by the inclusion Bayes factor and corresponding strength of evidence
Response accuracy	Stimulus Duration × Coherence	[a]	H_1, strong
Mean MT	Coherence		Inconclusive
	Stimulus duration		H_0, substantial
	Stimulus Duration × Coherence		H_0, anecdotal
Slope of muscle activation	Coherence	[a]	H_1, substantial
	Stimulus duration		H_0, substantial
	Stimulus Duration × Coherence		H_0, anecdotal
Mean PMT	Coherence	[a]	H_1, very strong
	Stimulus duration	[a]	H_1, decisive
	Stimulus Duration × Coherence		H_0, strong
Rate of PMA during the delay	EMG channel	[a]	H_1, decisive
Rate of PMA in the EMG channel associated with the response during the delay	Coherence	[a]	H_1, substantial
	Stimulus duration	[a]	H_1, decisive
	Stimulus Duration × Coherence		H_0, anecdotal

Note. Categories used to classify the strength of evidence correspond to those defined in the main text. MT = motor time; PMT = premotor time; PMA = partial motor activation; EMG = electromyography; GCD_{RS} = GCD extension for response signal tasks.
[a] Significant *p* value at the $\alpha = .05$ threshold level.

Table C3

Summary of Statistical Tests of GCD and GCD_{RS} Predictions (Experiment 3)

Dependent variable	Effect tested	*p* significance	Hypothesis favored by the inclusion Bayes factor and corresponding strength of evidence
Response accuracy (all blocks)	Coherence	[a]	H_1, decisive
	Block type	[a]	H_1, anecdotal
	Block Type × Coherence		H_0, anecdotal
Response accuracy (RS blocks)	Delay		H_0, strong
	Delay × Coherence		H_0, decisive
Mean MT (all blocks)	Block Type × Coherence	[a]	H_1, decisive
Mean MT (RS blocks)	Coherence	[a]	H_1, decisive
	Delay	[a]	H_1, very strong
	Delay × Coherence		H_0, strong
Slope of muscle activation (all blocks)	Block Type × Coherence	[a]	H_1, decisive
Slope of muscle activation (RS blocks)	Coherence	[a]	H_1, decisive
	Delay	[a]	H_1, very strong
	Delay × Coherence		H_0, strong
Mean PMT (all blocks)	Block Type × Coherence	[a]	H_1, decisive
Mean PMT (RS blocks)	Coherence		H_0, substantial
	Delay	[a]	H_1, very strong
	Delay × Coherence		H_0, substantial
Rate of PMA in the EMG channel associated with the response (FR blocks)	Coherence	[a]	H_1, decisive
Rate of PMA (RS blocks)	EMG Channel × Period	[a]	H_1, decisive

Note. Categories used to classify the strength of evidence correspond to those defined in the main text. RS = response signal; FR = free response; MT = motor time; PMT = premotor time; PMA = partial motor activation; EMG = electromyography; GCD = gated cascade diffusion model; GCD_{RS} = GCD extension for response signal tasks.
[a] Significant *p* value at the $\alpha = .05$ threshold level.

(*Appendices continue*)

Appendix D

Conditional Accuracy Functions Averaged Across Subjects for Each Condition of Experiment 1 (Panel A), Experiment 2 (Panel B), and Experiment 3 (Panel C)

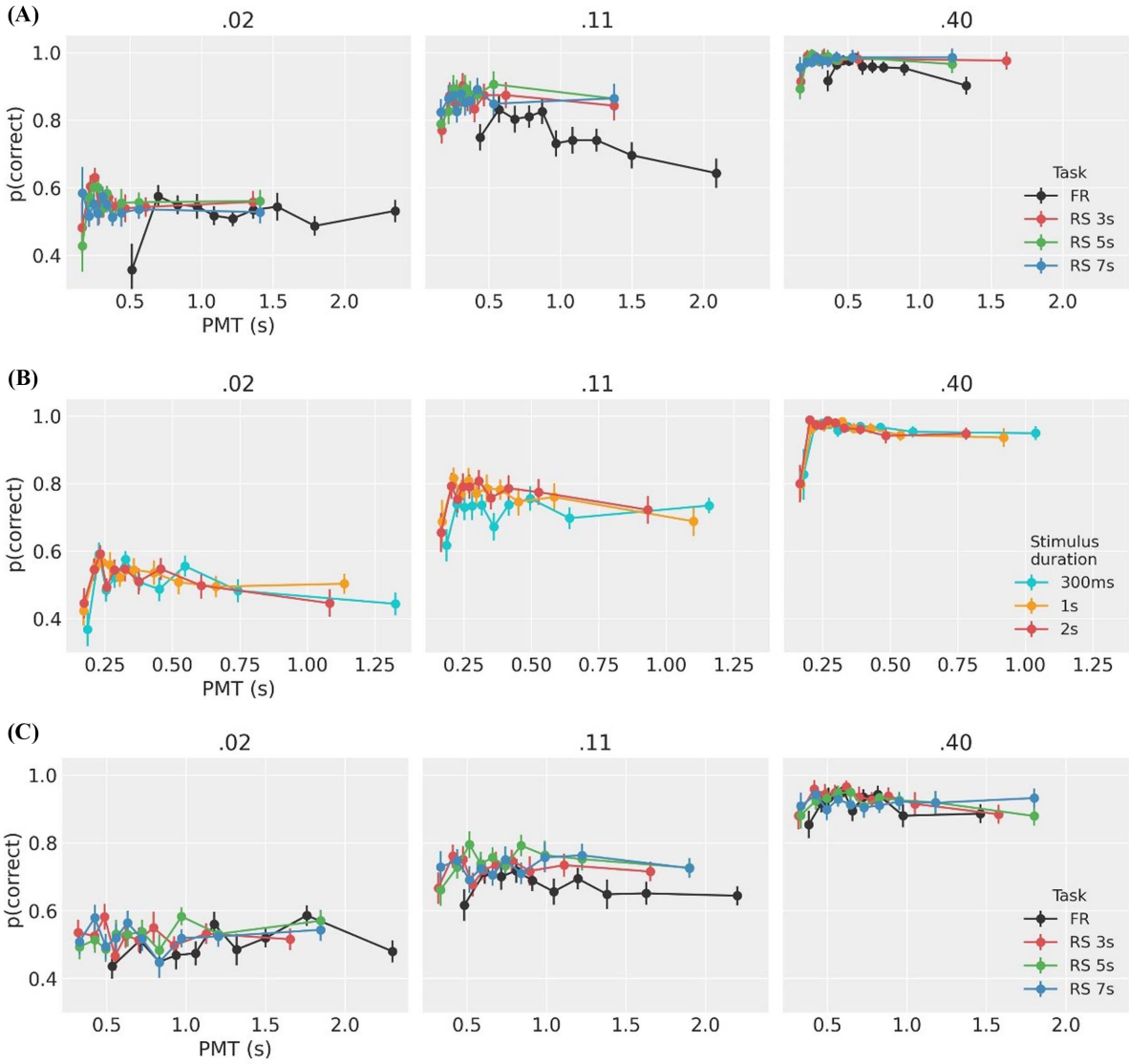

Note. Each conditional accuracy function was computed by plotting the proportion of correct responses (*y*-axis) as a function of the mean in each corresponding premotor time (PMT) bin. Ten PMT bins of equal size were chosen to provide a detailed window on conditional accuracy dynamics. RS = response signal; FR = free response. See the online article for the color version of this figure.

Received August 13, 2024
Revision received January 23, 2025
Accepted February 5, 2025 ■